MISCELLANEOUS PAPER GL-88-28

AXIAL RESPONSE OF THREE VIBRATORY AND THREE IMPACT DRIVEN H-PILES IN SAND

by

Larry M. Tucker, Jean-Louis Briaud

Briaud Engineers
1805 Laura Lane
College Station, Texas 77840

August 1988
Final Report

Prepared for US Army Engineer Division
Lower Mississippi Valley
Vicksburg, Mississippi 39180-0080

Under Contract No. DACW39-88-MO-421

Monitored by Geotechnical Laboratory
US Army Engineer Waterways Experiment Station
PO Box 631, Vicksburg, Mississippi 39180-0631

M.P. GL-88-28 AXIAL RESPONSE OF THREE VIBRATORY AND THREE IMPACT DRIVEN H-PILES IN SAND

Destroy this report when no longer needed. Do not return it to the originator.

The findings in this report are not to be construed as an official Department of the Army position unless so designated by other authorized documents.

The contents of this report are not to be used for advertising, publication, or promotional purposes. Citation of trade names does not constitute an official endorsement or approval of the use of such commercial products.

Unclassified

SECURITY CLASSIFICATION OF THIS PAGE

REPORT DOCUMENTATION PAGE

Form Approved OMB No. 0704-0188

1a. REPORT SECURITY CLASSIFICATION Unclassified	1b. RESTRICTIVE MARKINGS
2a. SECURITY CLASSIFICATION AUTHORITY	3. DISTRIBUTION/AVAILABILITY OF REPORT Approved for public release; distribution unlimited
2b. DECLASSIFICATION/DOWNGRADING SCHEDULE	
4. PERFORMING ORGANIZATION REPORT NUMBER(S)	5. MONITORING ORGANIZATION REPORT NUMBER(S) Miscellaneous Paper GL-88-28
6a. NAME OF PERFORMING ORGANIZATION Briaud Engineers 6b. OFFICE SYMBOL (If applicable)	7a. NAME OF MONITORING ORGANIZATION USAEWES Geotechnical Laboratory
6c. ADDRESS (City, State, and ZIP Code) 1805 Laura Lane College Station, TX 77840	7b. ADDRESS (City, State, and ZIP Code) PO Box 631 Vicksburg, MS 39180-0631
8a. NAME OF FUNDING/SPONSORING ORGANIZATION See Reverse 8b. OFFICE SYMBOL (If applicable) LMVD	9. PROCUREMENT INSTRUMENT IDENTIFICATION NUMBER Contract No. DACW39-88-MO-421
8c. ADDRESS (City, State, and ZIP Code) See Reverse	10. SOURCE OF FUNDING NUMBERS PROGRAM ELEMENT NO. / PROJECT NO. / TASK NO. / WORK UNIT ACCESSION NO.

11. TITLE (Include Security Classification)

Axial Response of Three Vibratory and Three Impact Driven H-piles in Sand

12. PERSONAL AUTHOR(S)
Tucker, Larry M.; Briaud, Jean-Louis

13a. TYPE OF REPORT	13b. TIME COVERED	14. DATE OF REPORT (Year, Month, Day)	15. PAGE COUNT
Final report	FROM _____ TO _____	August 1988	78

16. SUPPLEMENTARY NOTATION
Available from National Technical Information Service, 5825 Port Royal Road, Springfield, VA 22161

17. COSATI CODES			18. SUBJECT TERMS (Continue on reverse if necessary and identify by block number)
FIELD	GROUP	SUB-GROUP	Axial loading, Impact hammers, H-piles, Vibratory hammers

19. ABSTRACT (Continue on reverse if necessary and identify by block number)

A research program to compare the ultimate axial capacity of vibratory and impact driven H-piles in sand was conducted at a San Francisco, CA, site. The effects of time-lapse after driving was also studied. The piles were instrumented so that both pile tip loads and load transfer along the pile could be determined.

20. DISTRIBUTION/AVAILABILITY OF ABSTRACT ☒ UNCLASSIFIED/UNLIMITED ☐ SAME AS RPT. ☐ DTIC USERS	21. ABSTRACT SECURITY CLASSIFICATION Unclassified
22a. NAME OF RESPONSIBLE INDIVIDUAL	22b TELEPHONE (Include Area Code) / 22c. OFFICE SYMBOL

DD Form 1473, JUN 86 *Previous editions are obsolete.* SECURITY CLASSIFICATION OF THIS PAGE

Unclassified

8a. & 8c. NAME AND ADDRESS OF FUNDING/SPONSORING ORGANIZATIONS AND ADDRESSES (Continued).

US Army Engineer Division, Lower Mississippi Valley
PO Box 80
Vicksburg, MS 39180-0080

PREFACE

This report was prepared by Mr. Larry M. Tucker and Dr. Jean-Louis Briaud, College Station, Texas, under contract to the US Army Engineer Waterways Experiment Station (WES), Vicksburg, Mississippi, for the US Army Engineer Division, Lower Mississippi Valley. The report was prepared under Contract No. DACW39-88-MO-421.

This report was reviewed by Mr. G. Britt Mitchell, Chief, Engineering Group, Soil Mechanics Division (SMD), Geotechnical Laboratory (GL), WES. General supervision was provided by Mr. Clifford L. McAnear, Chief, SMD, and Dr. William F. Marcuson III, Chief, GL.

COL Dwayne G. Lee, EN, is Commander and Director of WES. Dr. Robert W. Whalin is Technical Director.

TABLE OF CONTENTS

LIST OF FIGURES

LIST OF TABLES

BACKGROUND

In the spring and summer of 1986 a series of vertical load tests were carried out on instrumented piles driven in sand at Hunter's Point in San Francisco. The Federal Highway Administration sponsored two projects on impact driven piles: one on the testing of five single piles and one on the testing of a five pile group (Ng, Briaud, Tucker 1988a; 1988b). Then, the Lower Mississippi Valley Division (LMVD) of the Corps of Engineers operating through the USAE Waterways Experiment Station (WES) sponsored a project on the comparison of impact driven piles and vibratory driven piles. Subsequently, the Deep Foundation Institute drove a number of piles with various vibratory hammers to compare the hammers' efficiencies.

This report is an analysis of the pile load tests sponsored by the LMVD through WES comparing impact and vibratory driven piles. The site is characterized, the load tests are described, the load tests results are analyzed and discussed, and recommendations and conclusions are made.

THE SOIL

The soil has been described in detail by Ng et al. (1988a). Below a 4 in thick asphalt concrete pavement is a 4.5 ft thick layer of sandy gravel with particles up to 4 inches in size. From 5 ft to 40 ft depth is a hydraulic fill made of clean sand (SP). Below 40 ft, layers of medium stiff to stiff silty clay (CH) are interbedded with the sand down to the bedrock. The fractured serpentine bedrock is found between 45 ft and 50 ft depth. The water table is 8 ft deep.

Many tests have been performed at the site including: standard penetration tests with a donut hammer and a safety hammer, sampling with a Sprague-Henwood sampler, cone penetrometer tests with point, friction and pore pressure measurements, preboring and selfboring pressuremeter tests, shear wave velocity tests, dilatometer tests and stepped-blade tests. The CPT, SPT and stepped-blade tests were performed before and after driving and testing of the FHWA test piles. The location of selected soundings are shown on Figure 1. The corresponding profiles are shown on Figures 2 through 7. The hydraulic fill has the following average properties:

Friction angle	32^{o} to 35^{o}
Water content	22.6 %
Dry unit weight	100 pcf
D_{60}	0.8 mm
D_{10}	0.7 mm
SPT blow count	15 bpf
CPT tip resistance	65 tsf
PMT net limit pressure	7 tsf
Shear modulus (from shear wave velocity measurements)	400 tsf

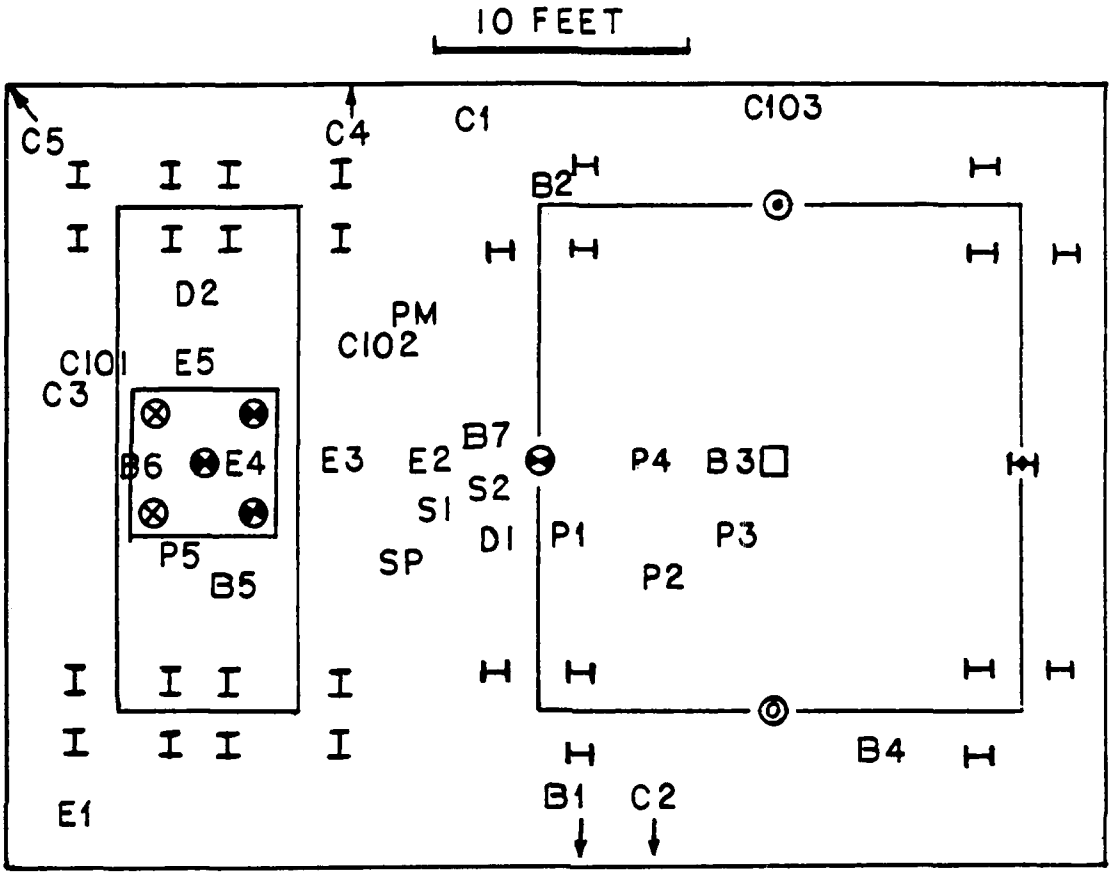

S	STEP BLADE TESTS
B	SPT TEST BORINGS
C	CONE PENETROMETER TESTS
D	DILATOMETER TESTS
E	EXTENSOMETER
P	PIEZOMETER
PM	PREBORING PRESSUREMETER TESTS
SP	SELFBORING PRESSUREMETER TESTS

Figure 1. Location of Borings and Instrumentation

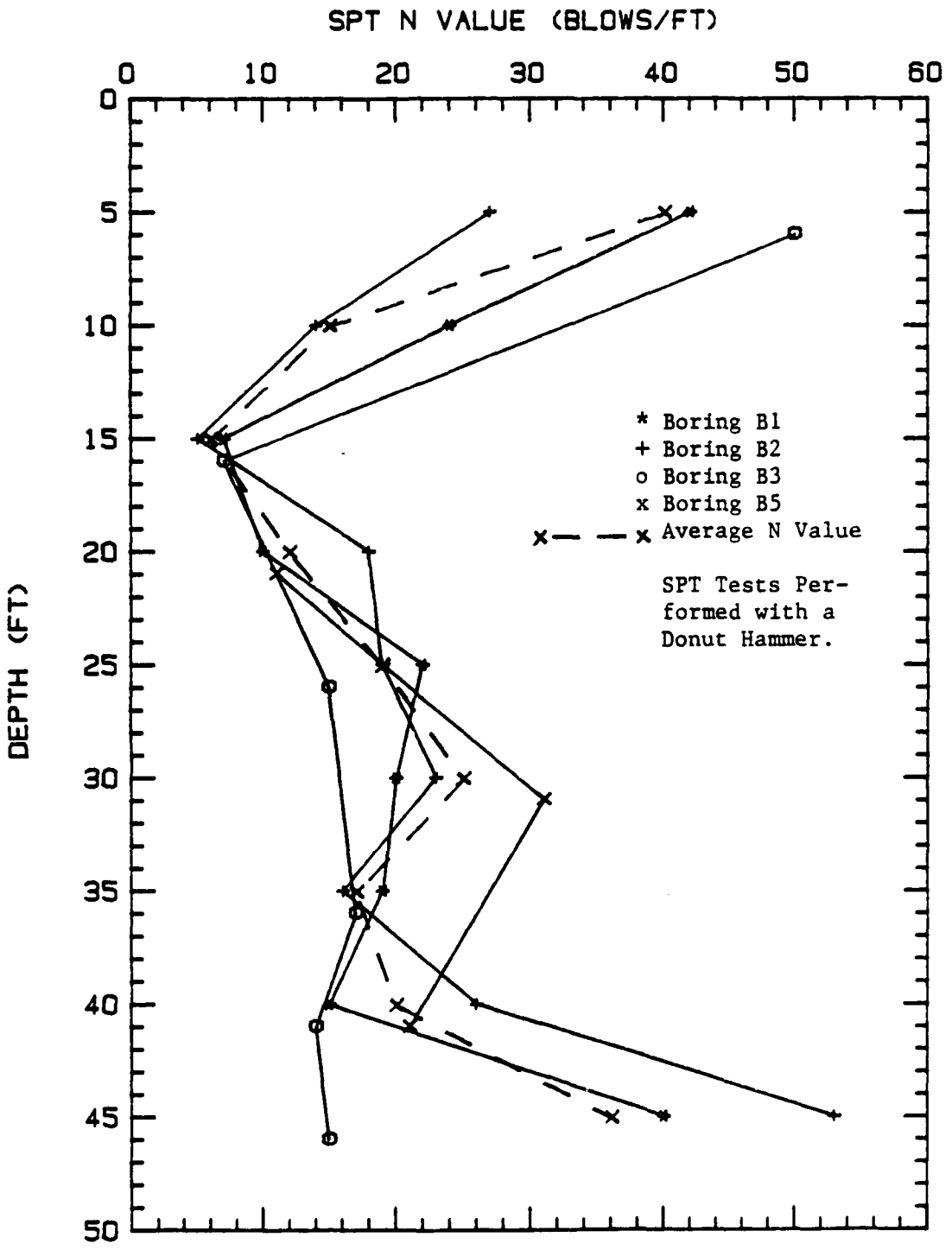

Figure 2. Profiles of Standard Penetration Test Blowcounts

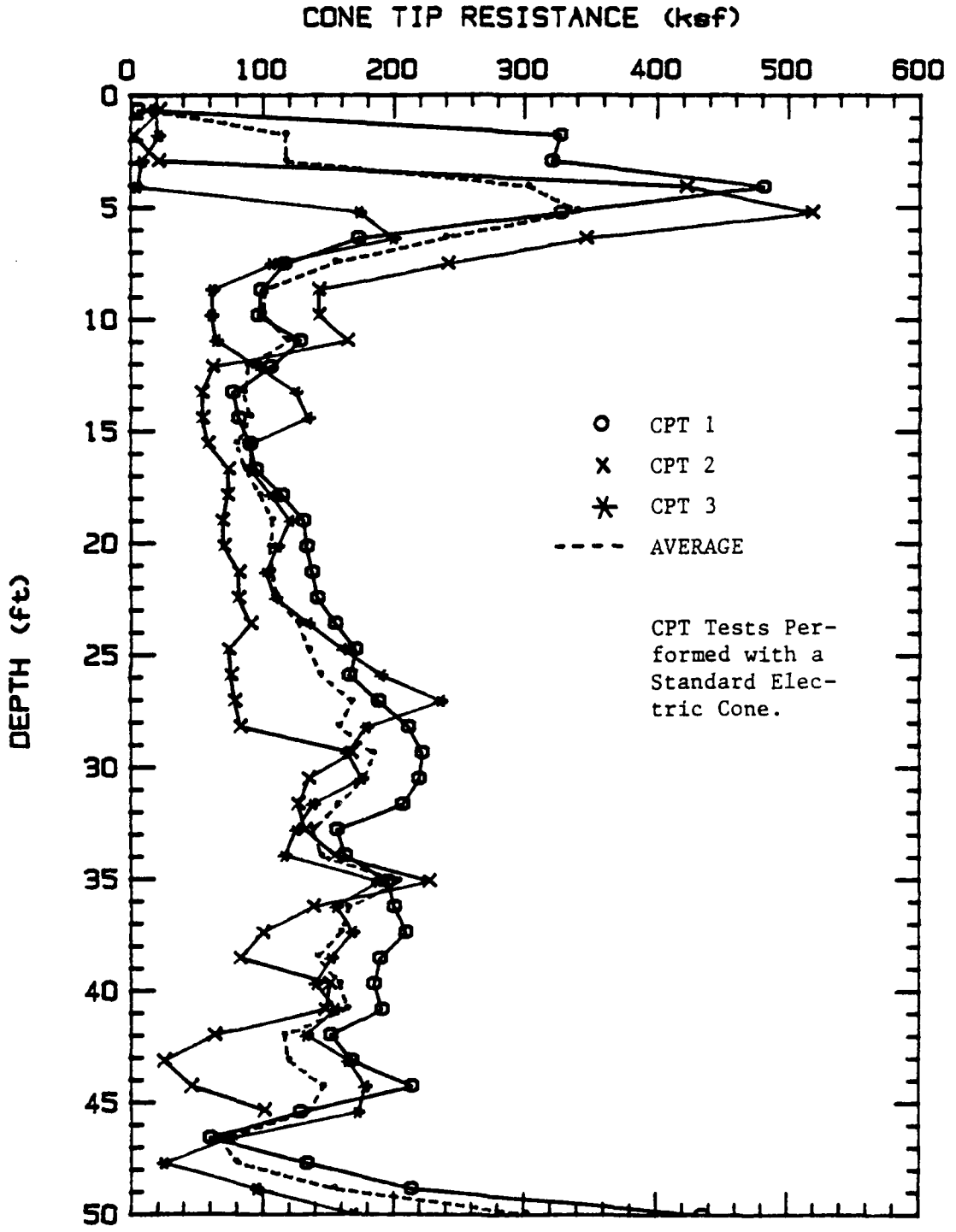

Figure 3. CPT Profiles for Point Resistance

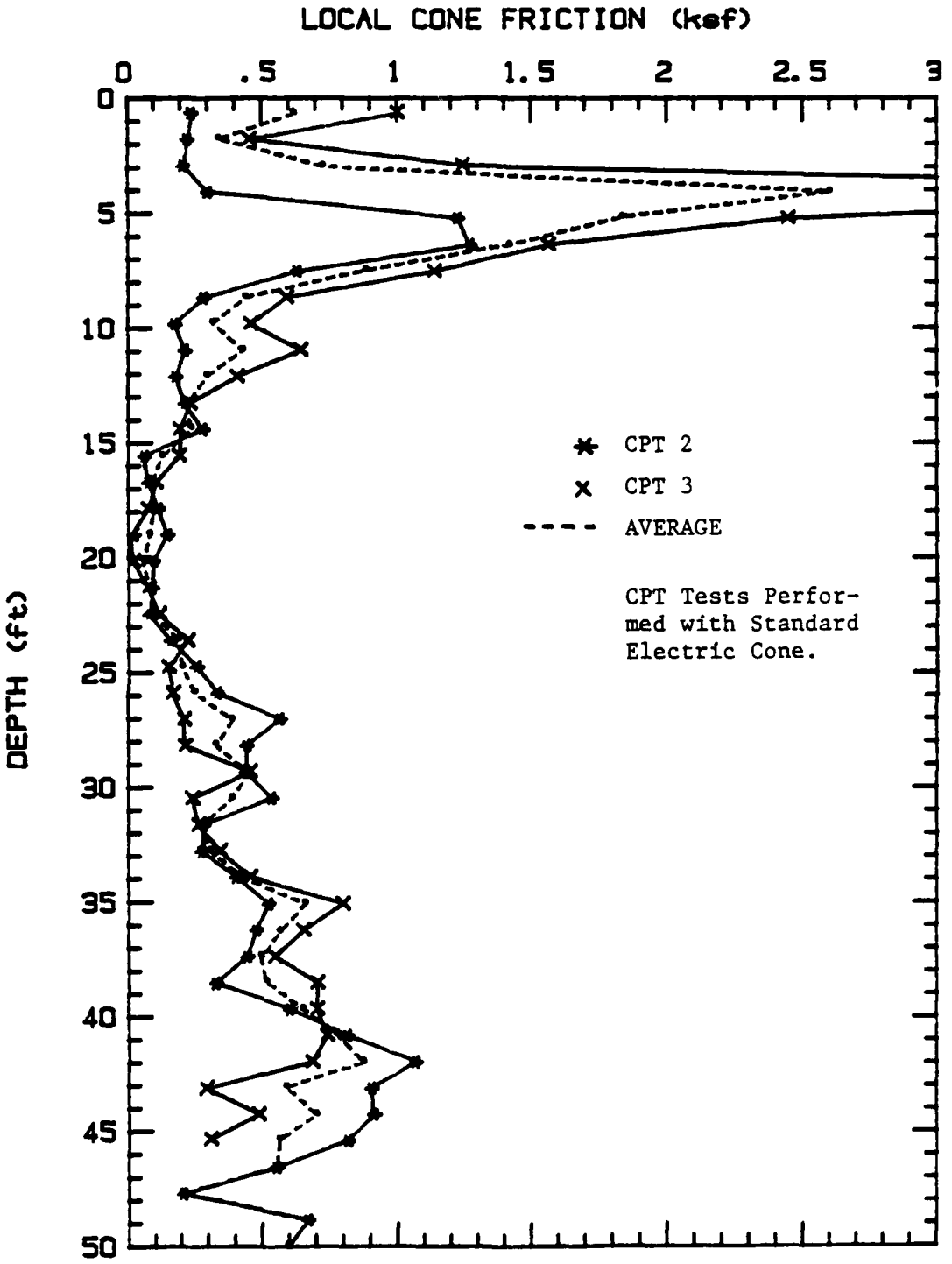

Figure 4. CPT Profiles for Friction Resistance

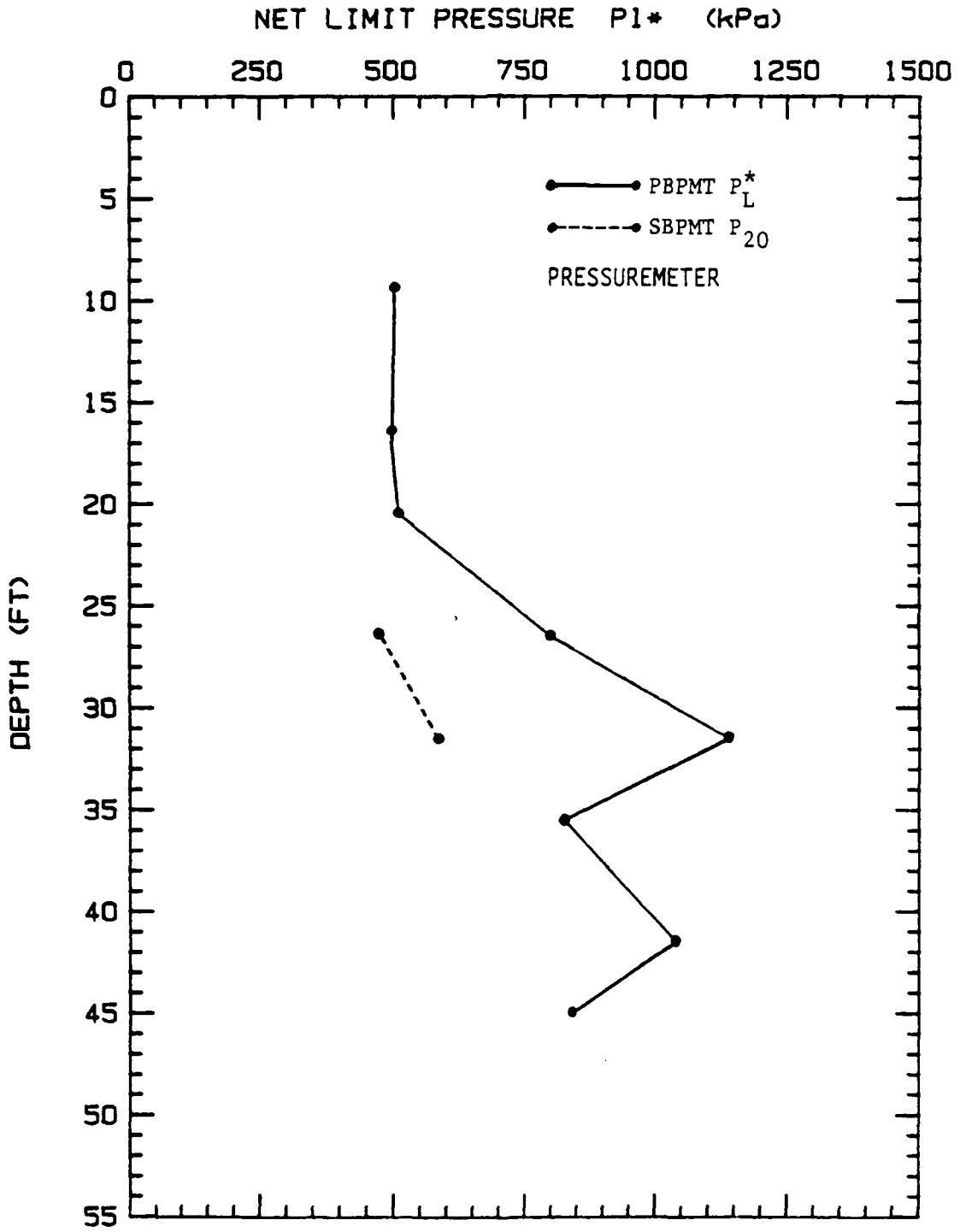

Figure 5. Net Limit Pressure Profile

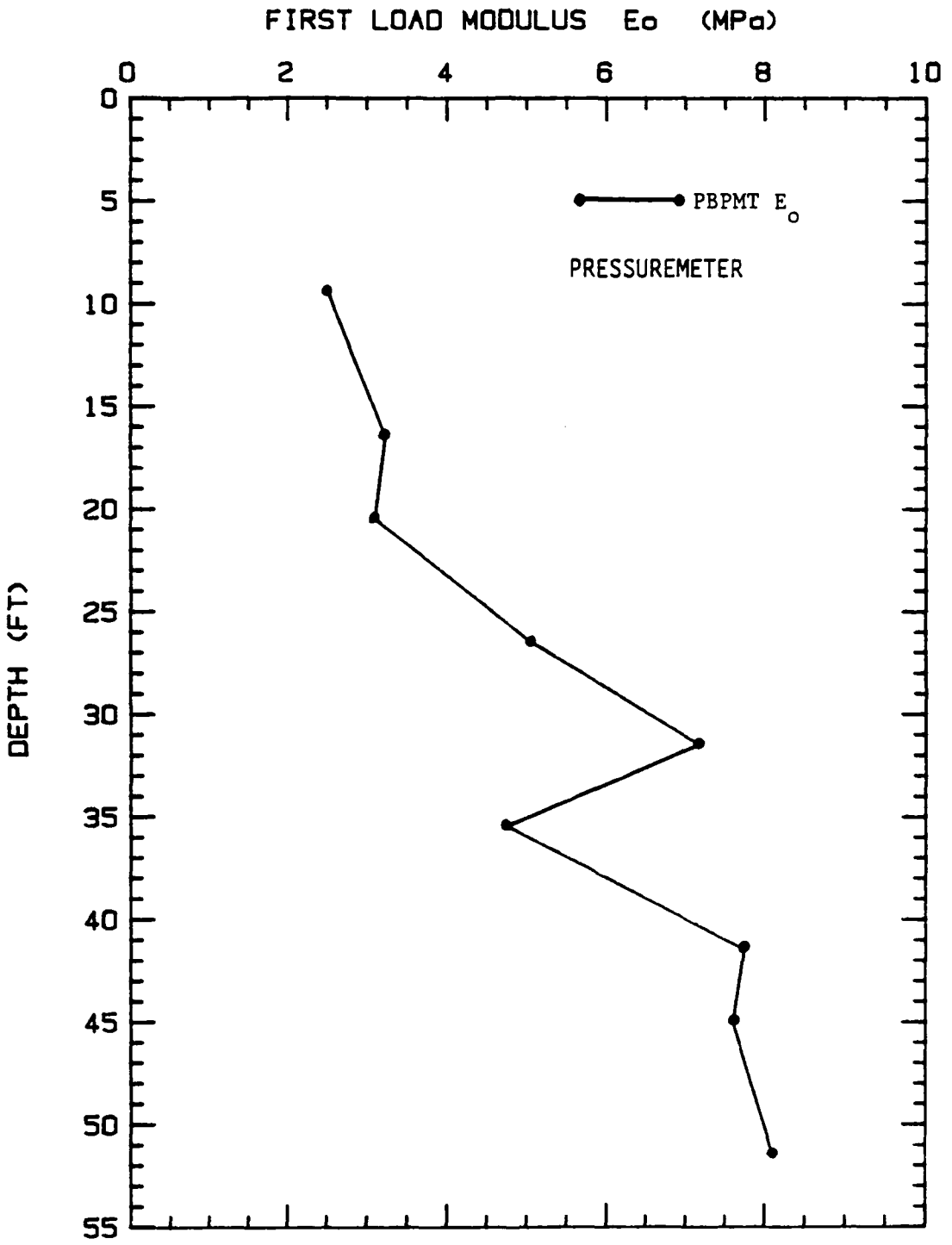

Figure 6. First Load Modulus Profile

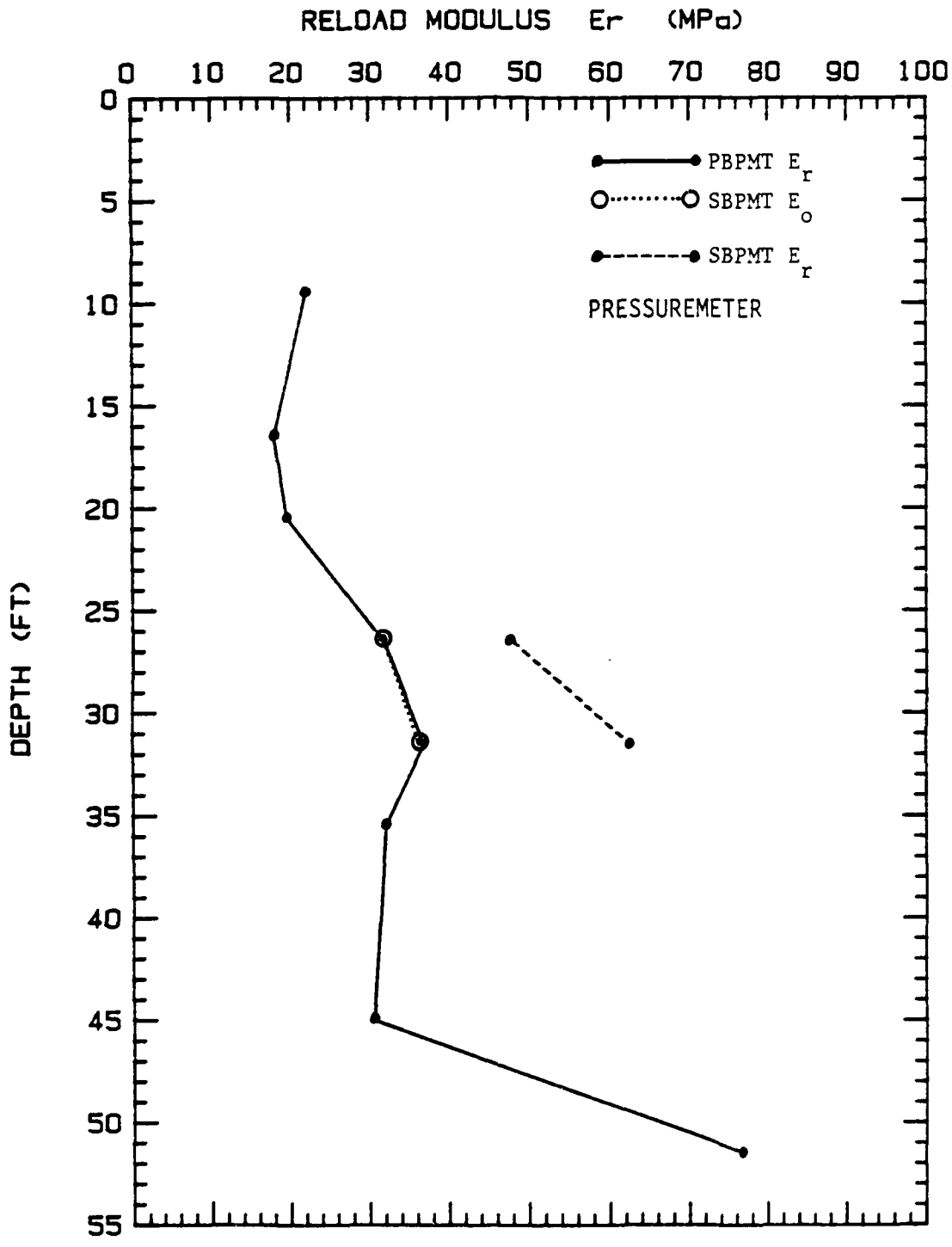

Figure 7. Reload Modulus Profile

THE PILES AND LOAD TEST PROCEDURES

Three HP14x73 steel H piles were used in this program. They were all embedded 30 ft below the ground surface; however, a 4.5 ft deep, 14 in diameter hole was drilled prior to pile insertion for the impact driven piles, making the true pile embedment equal to 25.5 ft. For the vibratory driven piles a hole was drilled through the 4 in thick asphalt layer only, making the embedment equal to 29.5 ft. Each pile had two angles (2.5 x 2.5 x 3/16 inches) welded to the sides of the pile web as protection for the instrumentation.

The first pile was one of the single piles used in the FHWA program (referred to as pile 1). Pile 1 was instrumented with seven levels of strain gauges and a tell tale at the pile tip (Figure 8). This pile was calibrated before driving and the pile stiffness was measured for use in the data reduction. The measured value of pile stiffness (AE) was 614908 kips. This value was used for all three piles. Pile driving analyzer measurements were obtained during the driving of pile 1 with an impact hammer. Pile 1 was then load tested in compression 30 days after it was driven (FHWA program): this is load test 1I. Pile 1 was then retested at 67 days after driving: this is load test 1IR. After pile 1 was retested, the pile was restruck with an impact hammer and pile driving analyzer measurements were obtained. Pile 1 was then extracted and vibrodriven about 30 ft from the impact test (Figure 9). It was load tested at 33 days after driving (load test 1V) and again at 63 days after driving (load test 1VR). After load test 1VR the pile was struck with an impact hammer and pile driving analyzer measurements were obtained.

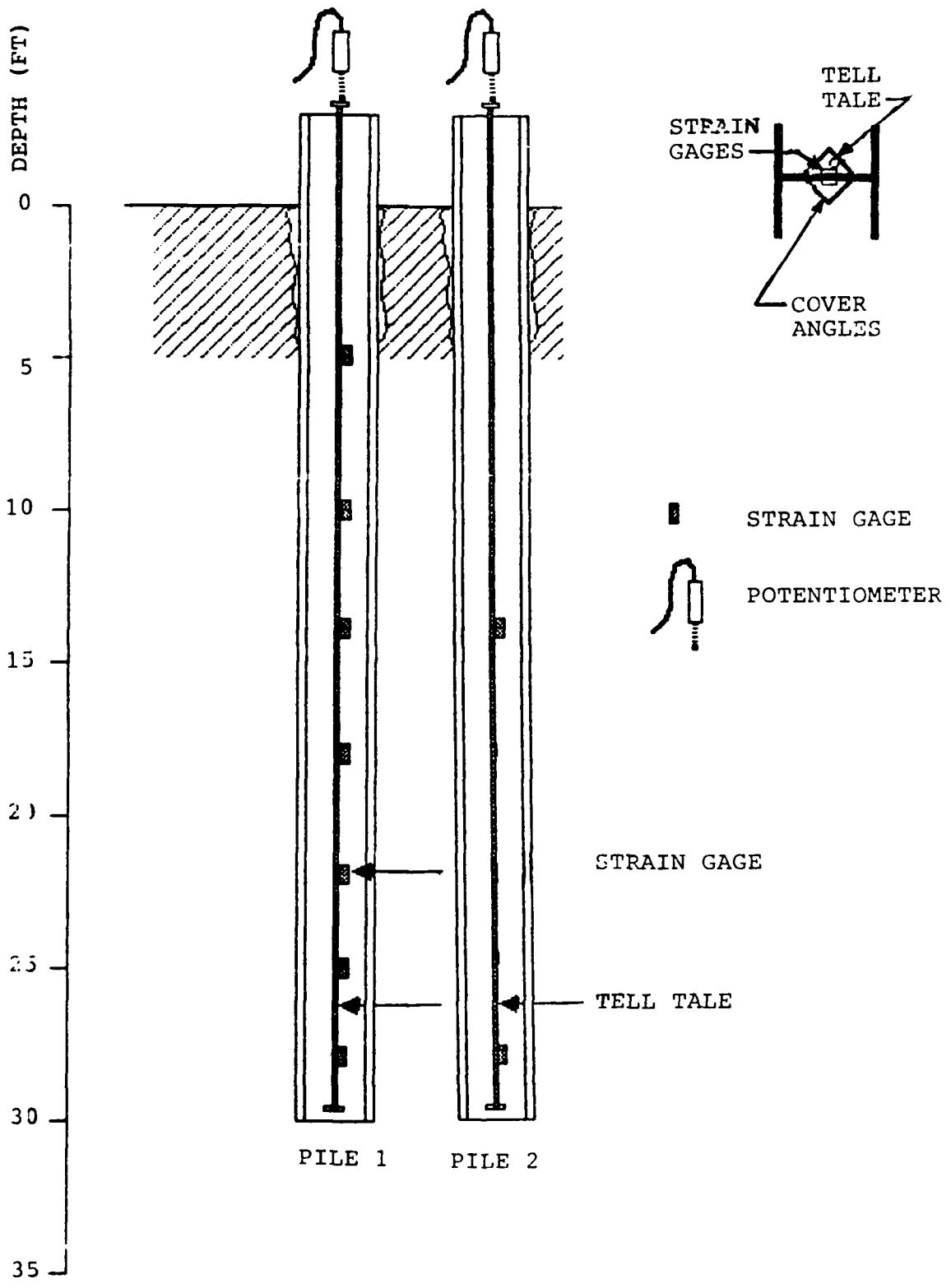

Figure 8. Location of Pile Instrumentation

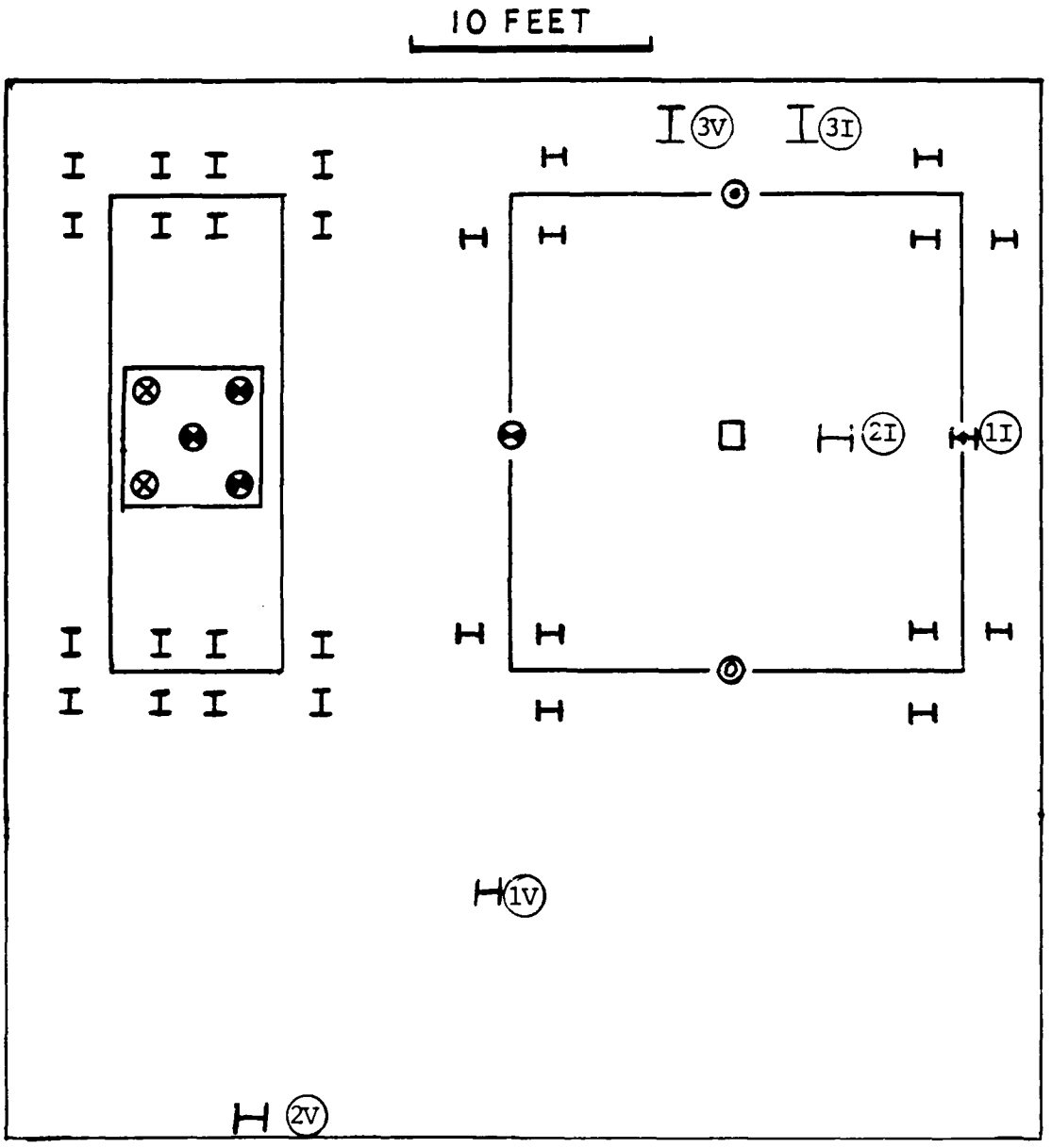

Figure 9. Test Pile Locations

The second pile (Pile 2) was instrumented with two levels of strain gauges: one at the mid-point and one at the pile tip (Figure 8). Pile 2 was impact driven and tested at 65 days after driving: this is load test 2I. Pile 2 was then extracted and vibrodriven and tested at 64 days after driving. This is load test 2V. After load test 2V, the pile was struck with an impact hammer and pile driving analyzer measurements were obtained.

The third pile (Pile 3) was not instrumented. It was impact driven and tested at 12 days after driving: this is load test 3I. Pile 3 was then extracted and vibrodriven. It was tested at 12 days after driving: this is load test 3V. Table 1 summarizes the eight load tests presented in this report.

The impact driven piles were installed using a Delmag D22 diesel hammer at full throttle. All restrike measurements were also obtained using this hammer. The hammer was rated at approximately 40,000 ft-lbs maximum energy. Details of the hammer are given in Table 2. The driving records for the impact driven piles are shown in Figure 10.

The vibratory driven piles were installed with a ICE-216 vibratory hammer. Details of the hammer are given in Table 3. The penetration rates versus depth records for these piles are shown in Figure 11.

The load test procedure has been described in detail by Ng et al. (1988). In general, the test loads were applied in increments of 10 percent of the estimated ultimate load. Each load step was held for at least 30 minutes, with the load being monitored continuously. All readings from electronically monitored instruments were recorded every 5 minutes. The data was stored on floppy disk for data reduction.

Table 1. Load Test Program Summary

Test Piles

1I	-	FHWA Pile (Impact)	30 Day test
1IR	-	FHWA Pile (Impact)	67 Day test
1V	-	FHWA Pile (Vibratory)	33 Day test
1VR	-	FHWA Pile (Vibratory)	63 Day test
2I	-	New Pile (Impact)	65 Day test
2V	-	New Pile (Vibratory)	64 Day test
3I	-	New Pile (Impact)	12 Day test
3V	-	New Pile (Vibratory)	13 Day test

Notes:

A. 1I, 1IR, 1V and 1VR - Seven strain gauge levels

B. 2I and 2V - Two strain gauge levels

C. 3I and 3V - No strain gauges

Table 2. Specifications for Delmag D22 Impact Hammer

Rated energy	39,700 ft-lbs
Ram weight	4,850 lbs
Blows/minute	42-60
Maximum explosive pressure on pile	158,700 lbs
Working weight	11,275 lbs
Drive Cap weight	1,500 lbs

Table 3. Specifications for ICE-216 Vibratory Driver

Eccentric moment	1000 in-lbs
Frequency	400-1600 vpm
Amplitude	1/4 - 3/4 inches
Power	115 HP
Pile clamping force	50 tons
Line pull for extraction	30 tons
Suspended weight with clamp	4825 lbs
Length	47 inches
Width	16 inches
Throat width	12 inches
Height with clamp	78 inches
Height without clamp	68 inches

PENETRATION (ft)	BLOWCOUNT (blows/ft) PILE 1	PILE 2	PILE 3
1	RUN	NA*	RUN
2			
3			
4			
5			
6			
7			
8			
9	2		
10	1		4
11	2		4
12	2		4
13	3		4
14	2		4
15	2		4
16	2		4
17	2		5
18	2		4
19	2		4
20	2		6
21	2		6
22	4		6
23	6		6
24	5		8
25	7		8
26	7		9
27	8		10
28	10		9
29	11		11
30	12		11
TOTAL	96		131

* Not available

Figure 10. Impact Pile Driving Records

Depth (ft)	Pile 1		Pile 2		Pile 3	
	Time (sec)	Rate of Penetration (ft/min)	Time (sec)	Rate of Penetration (ft/min)	Time (sec)	Rate of Penetration (ft/min)
0						
1						
2						
3						
4						
5	1.9					
6						
7	6.7	25.0				
8						
9					4	15
10			12	10	9	12
11	12.2	43.6	18	12	14	12
12			23	12	19	12
13	16.8	26.1	28	10	23	15
14	22.7	10.2	34	12	29	10
15	28.4	10.5	39	12	34	12
16	34.6	9.7	44	12	38	15
17	39.0	13.6	49	12	42	15
18	45.1	9.8	54	12	46	15
19			58	15	49	20
20			63	12	53	15
21	57.2	14.9	66	20	58	12
22	61	15.8	69	20		
23			73	15	61	40?
24			76	20	64	20
25	70	20	79	20	67	20
26			83	15	70	20
27			86	20	73	20
28			89	20	76	20
29			92	20	80	15
30	85	20	96	15	85	12

Figure 11. Vibratory Pile Driving Records

LOAD TEST RESULTS

Residual Stresses

Residual driving stresses were measured for pile 1I. The stress profile was not monitored between load test 1I and test 1IR. Therefore the residual stress profile after driving was also used for load test 1IR. Since additional residual stresses are usually induced due to a compression test, this profile is slightly in error. The residual stress profile is the first load profile shown in Figure 14.

An attempt was made to record the residual driving stresses for pile 2I. However, the readings obtained were judged unreliable. Therefore, the residual stress profile from pile 1I was used in reducing the load test data for pile 2I (Figure 14).

The vibratory driven piles were assumed to have no residual driving stresses. No attempt was made to verify this. However, published data substantiate this assumption (Hunter and Davisson, 1969).

Load Test Results

The raw data from the floppy disks was reduced to obtain the following information:

Load-settlement curve at the pile top

Load versus depth profiles - a. raw data
b. including residual loads
c. interpreted profile

Load transfer curve (friction and point)

The number of plots possible for a given load test depends upon the amount of instrumentation on the pile.

As stated above, three sets of load versus depth profiles are plotted for those piles instrumented with strain gauges. The first set of

profiles will be the raw data as measured during the test. Since all instrumentation was zeroed just before the load test, these profiles do not include residual stresses.

A second set of profiles is shown for those piles driven with an impact hammer which include the residual loads in the pile due to driving. This set of profiles is not shown for the vibratory driven piles since it has been assumed that no residual stresses are induced due to installation.

The third set of profiles is the interpreted load versus depth curves. The measured data shows some irregularities which may be due to drift in the readings, temperature fluctuation or gauge malfunction. A gauge reading was omitted entirely if it was known that the gauge was definitely malfunctioning. This was the case with the gauge at a depth of 25 ft for pile 1V and 1VR, and for both gauge levels on pile 2V. Any other irregularities were smoothed by fitting a second order polynomial curve through the data. These curves are shown as the third set of load versus depth profiles. Other interpretations are obviously possible. However, the fit of the curves matches quite well with what one would draw manually.

The results for load test 1I are given in Figures 12 through 17; load test 1IR results are shown in Figures 18 through 23; load test 1V results are shown in Figures 24 through 28; load test 2VR results are shown in Figures 29 through 33; load test 2I results are shown in Figures 34 through 39. Load-settlement curves at the pile top are shown in Figures 40 through 42 for load tests 2V, 3I and 3V respectively.

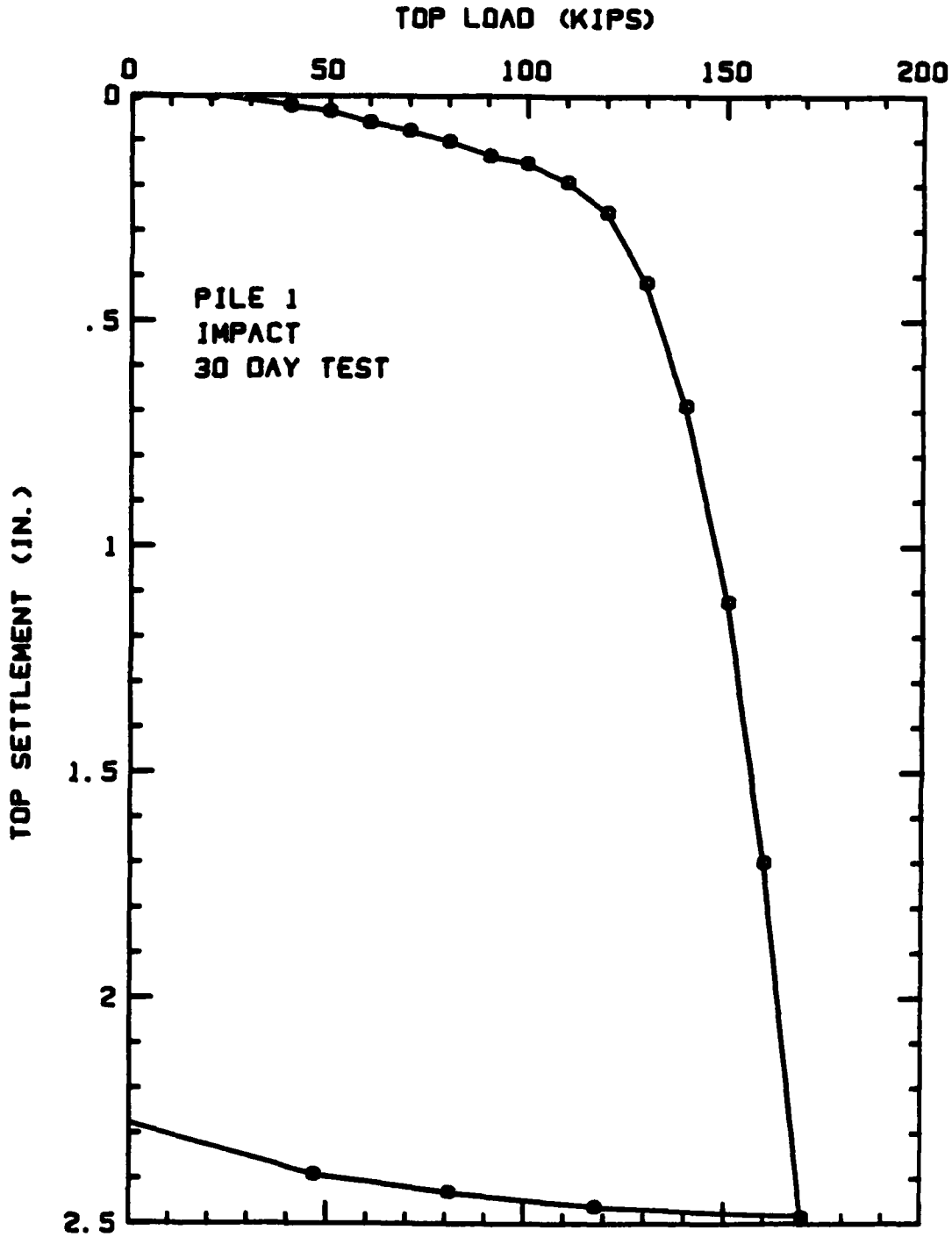

Figure 12. Load-Settlement Curve for Pile 1I

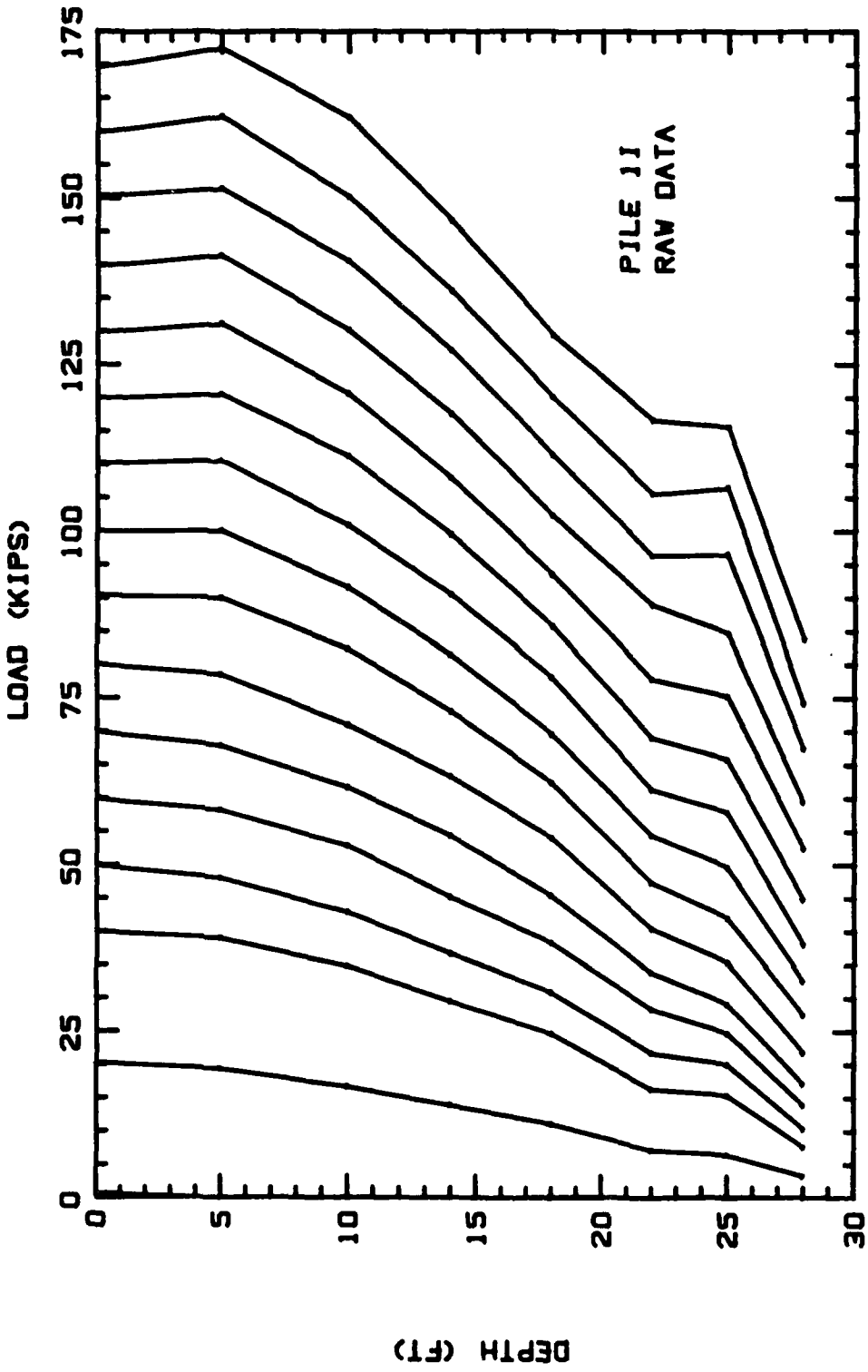

Figure 13. Raw Load Versus Depth Profiles for Pile 11

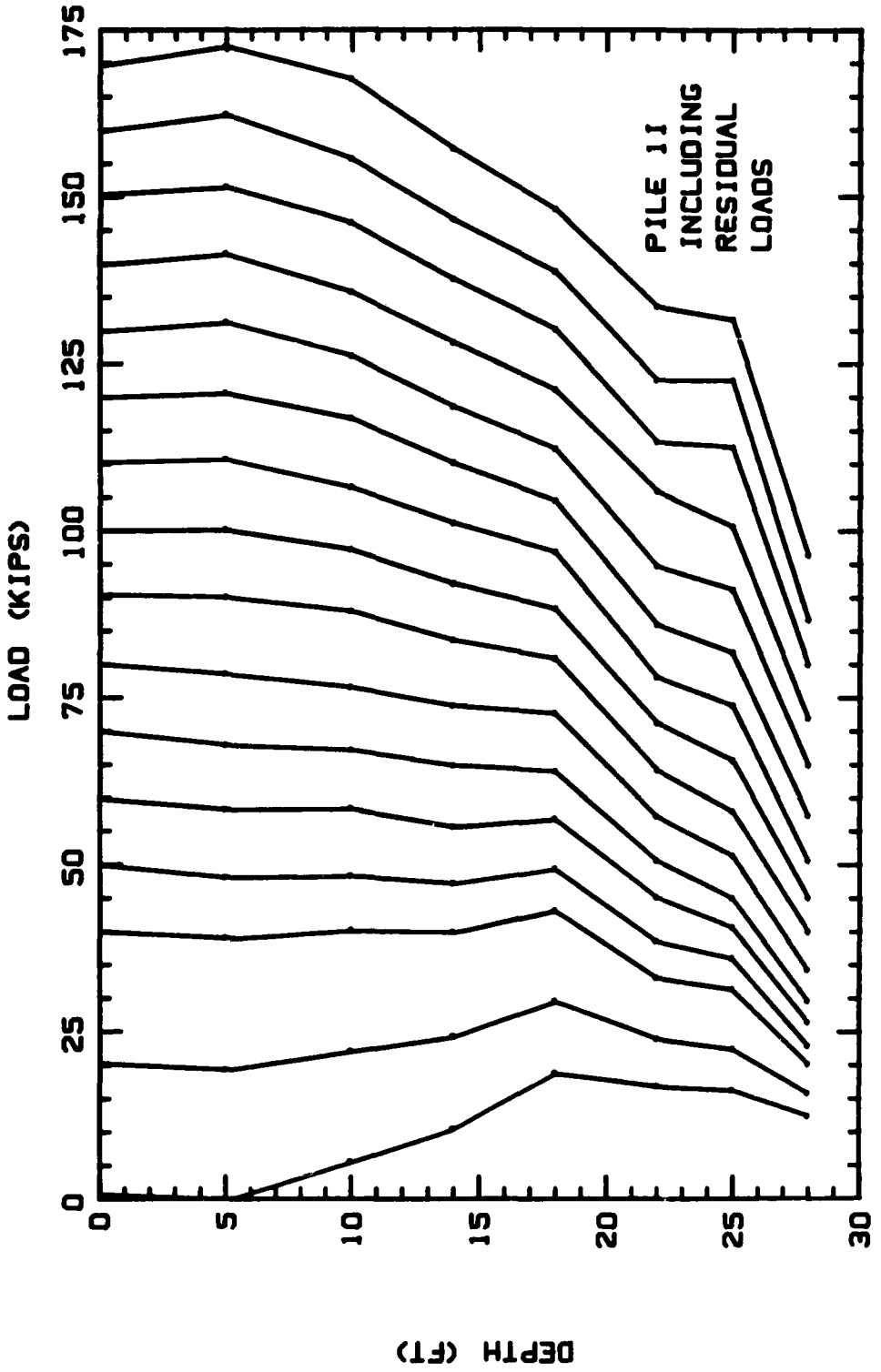

Figure 14. Corrected Load Versus Depth Profiles for Pile 11

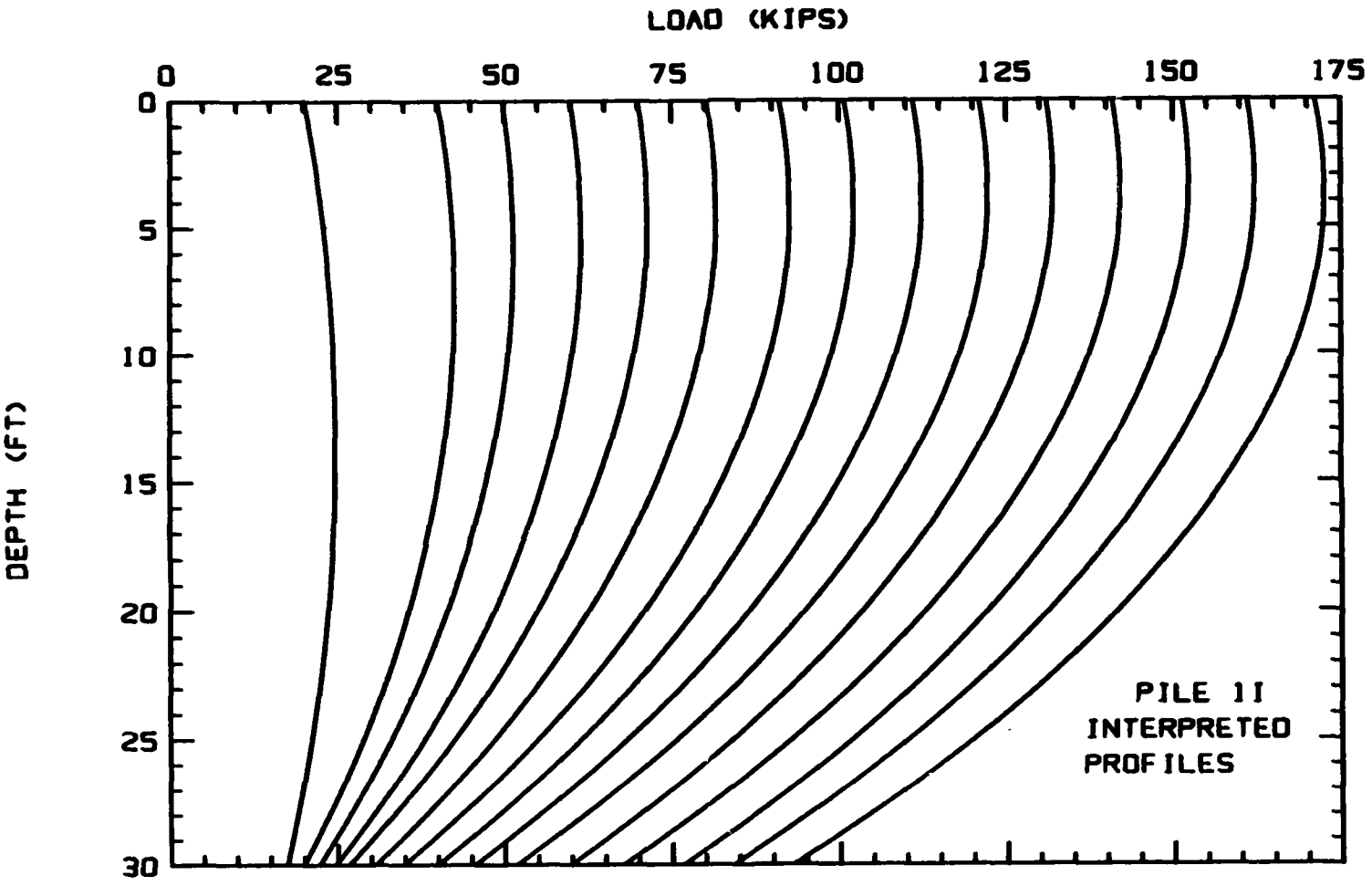

Figure 15. Interpreted Load Versus Depth Profiles for Pile 1I

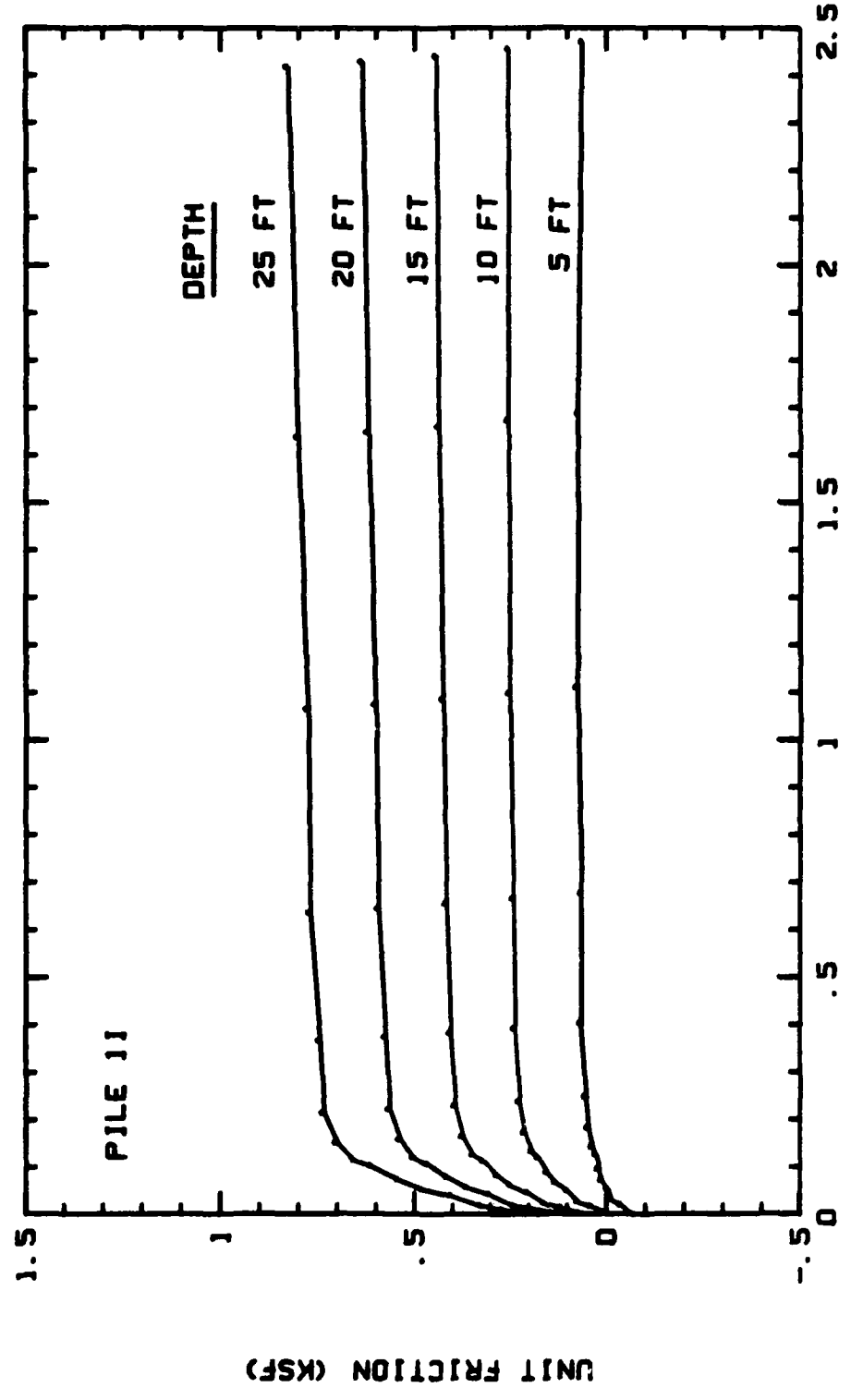

Figure 16. Friction Versus Movement Curves for Pile 11

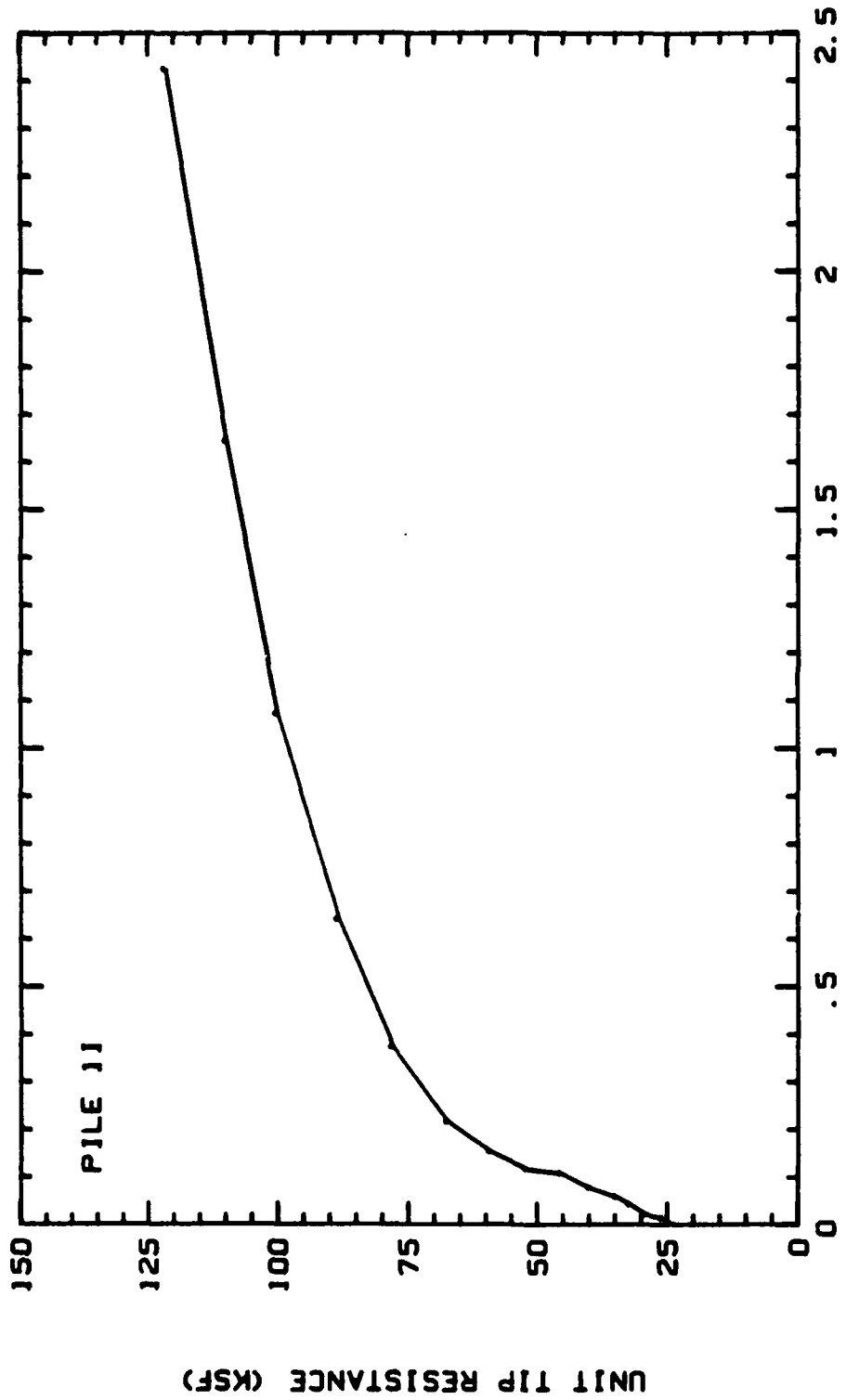

Figure 17. Point Resistance Versus Movement Curve for Pile 11

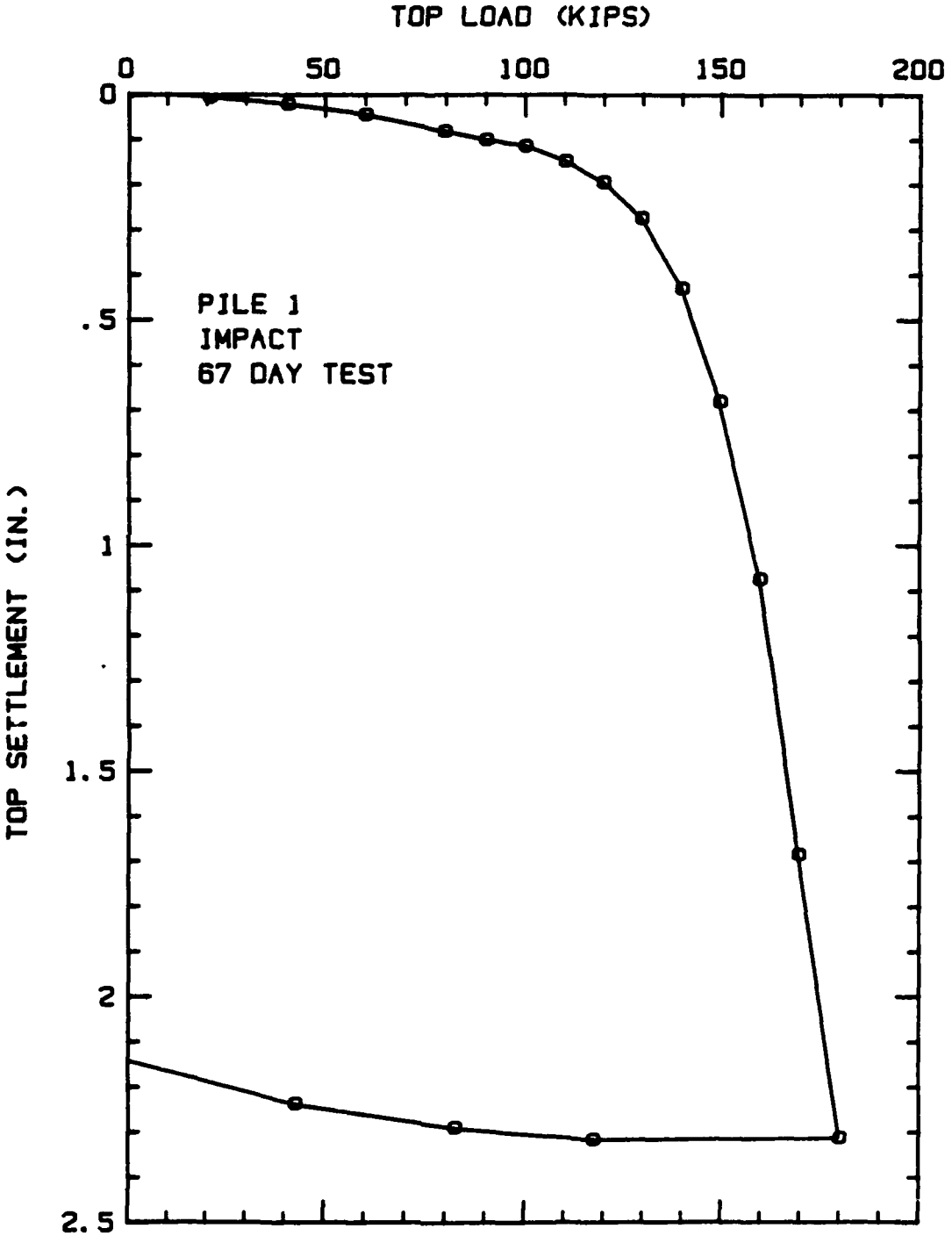

Figure 18. Load-Settlement Curve for Pile 1IR

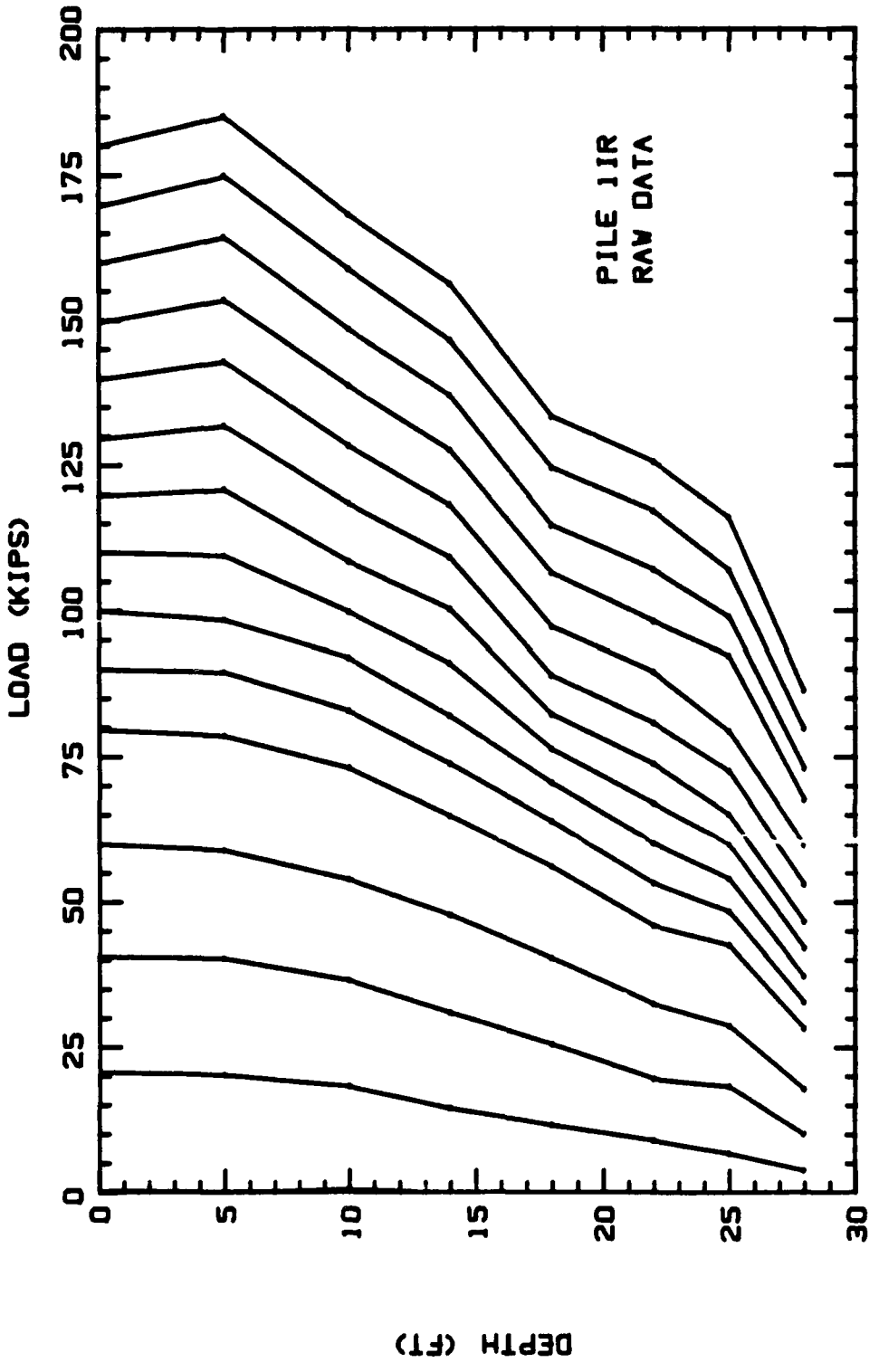

Figure 19. Raw Load Versus Depth Profiles for Pile 1IR

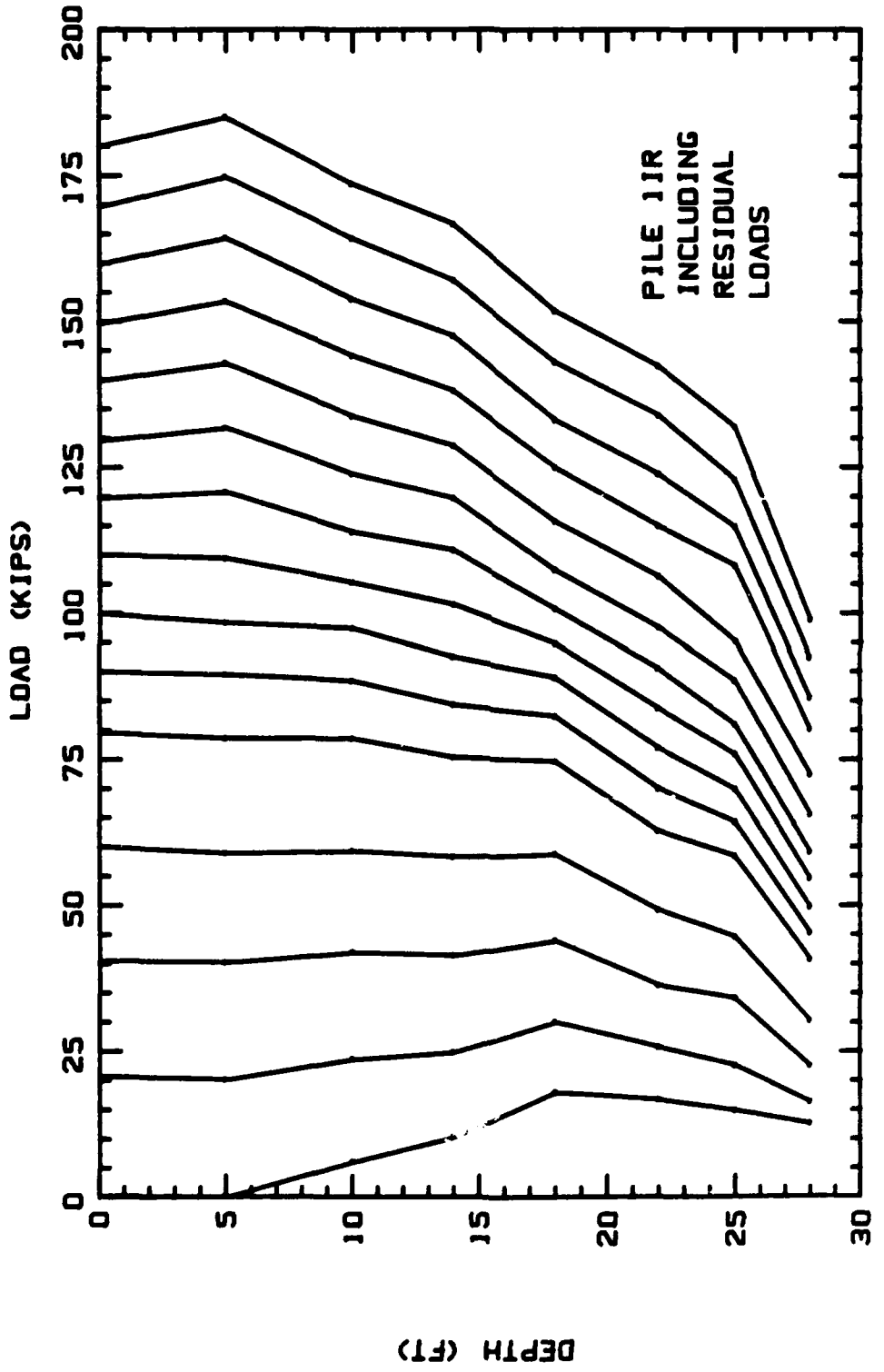

Figure 20. Corrected Load Versus Depth Profiles for Pile 1IR

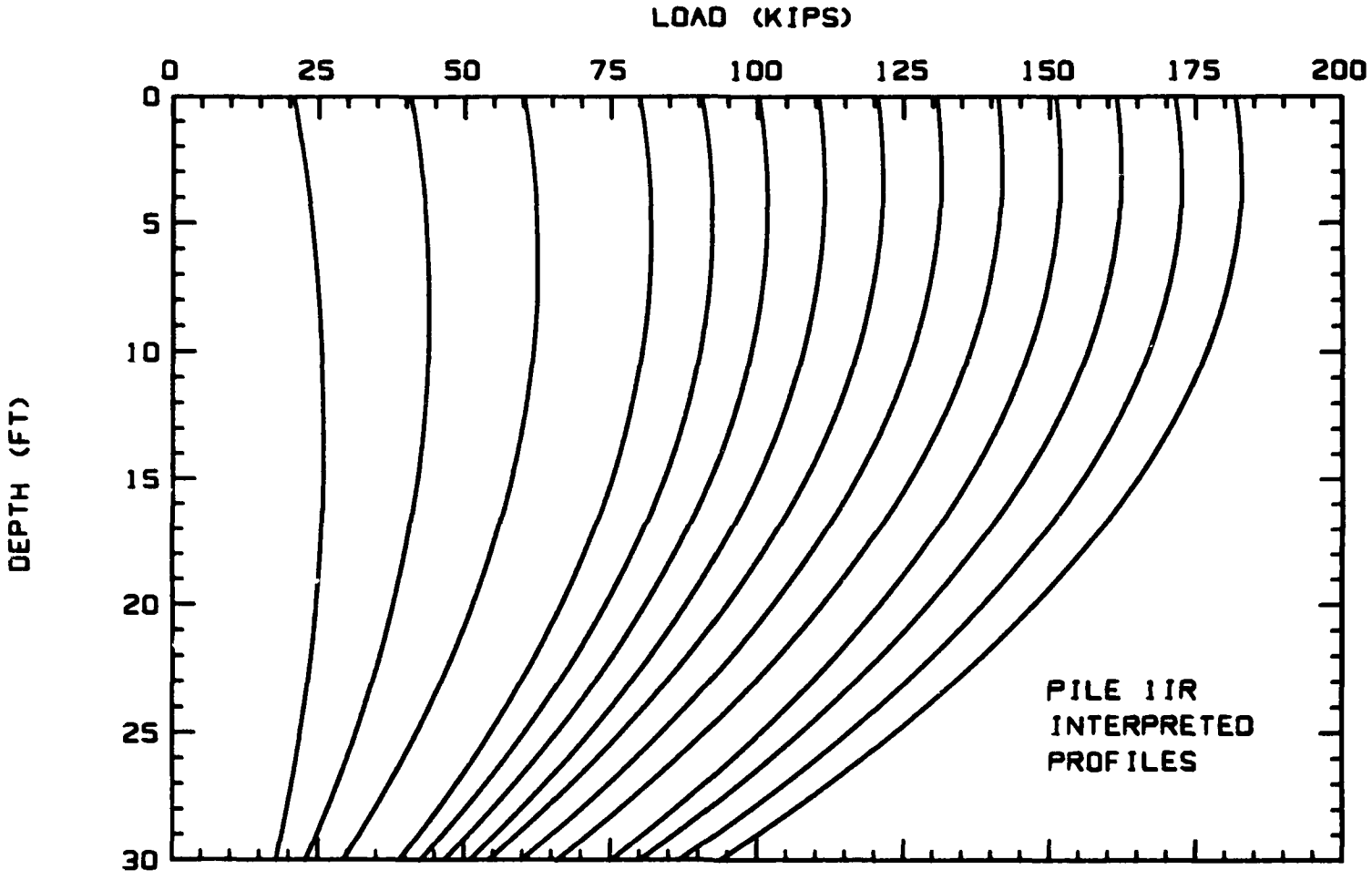

Figure 21. Interpreted Load Versus Depth Profiles for Pile 11R

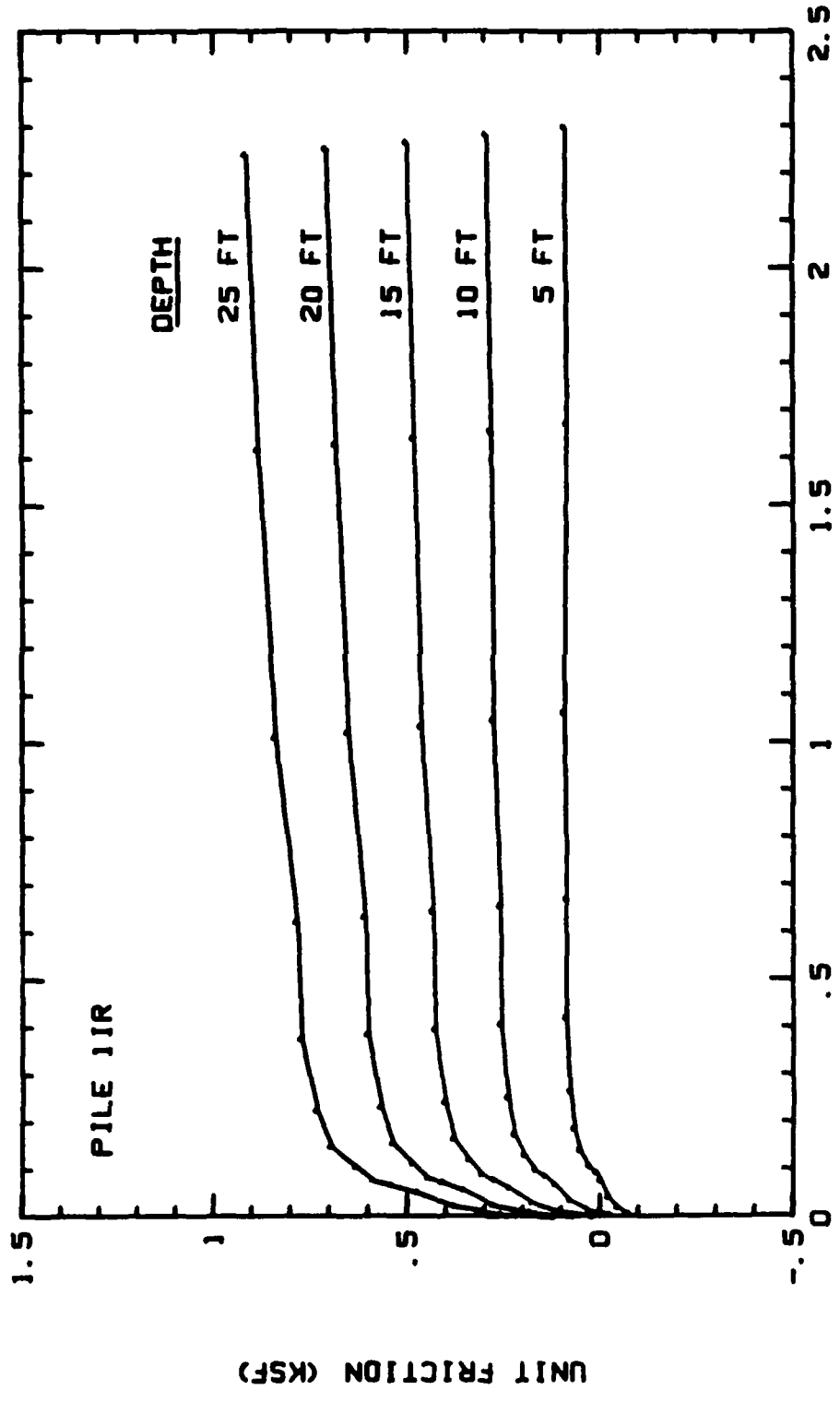

Figure 22. Friction Versus Movement Curves for Pile 1IR

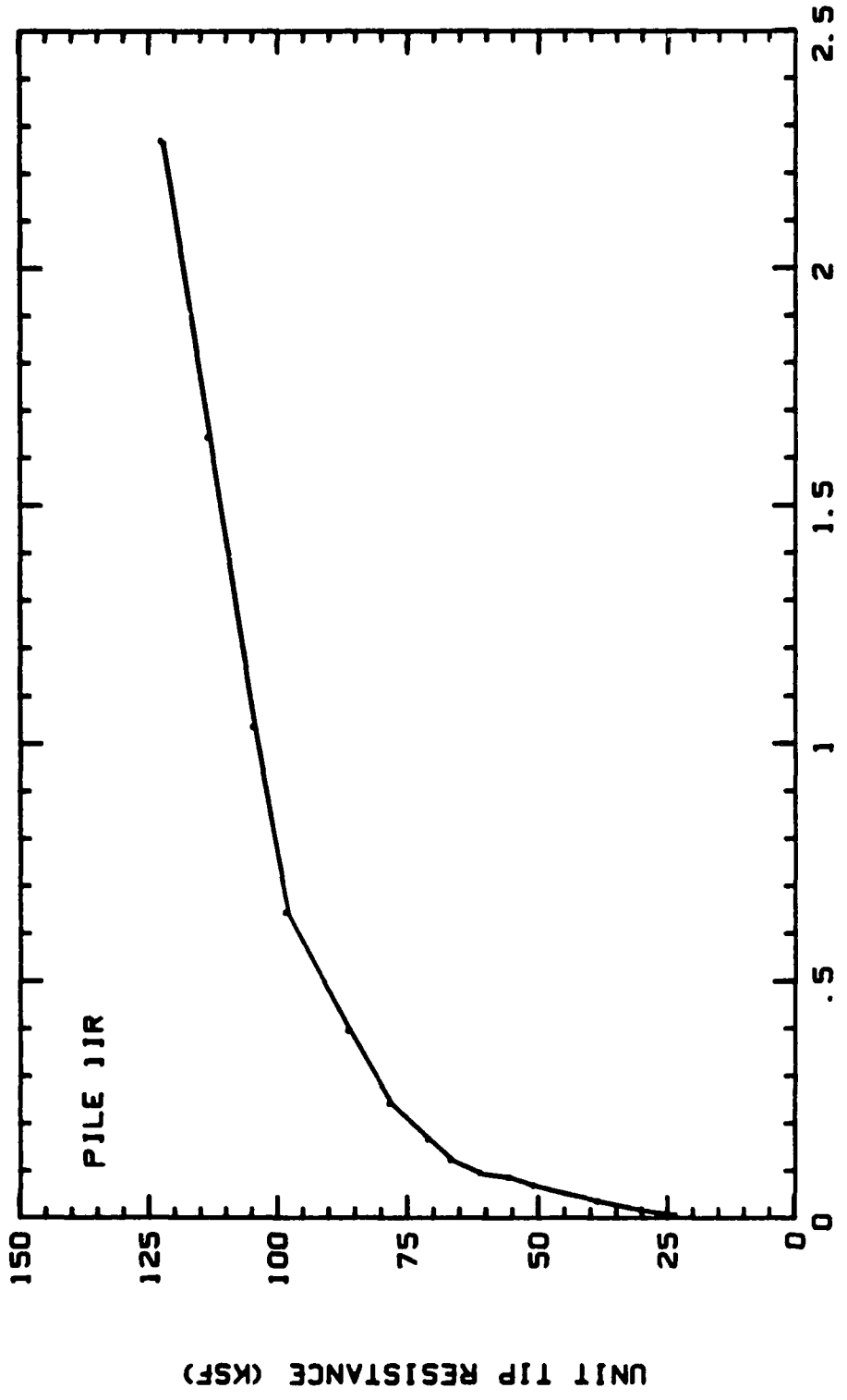

Figure 23. Point Resistance Versus Movement Curve for Pile 1IR

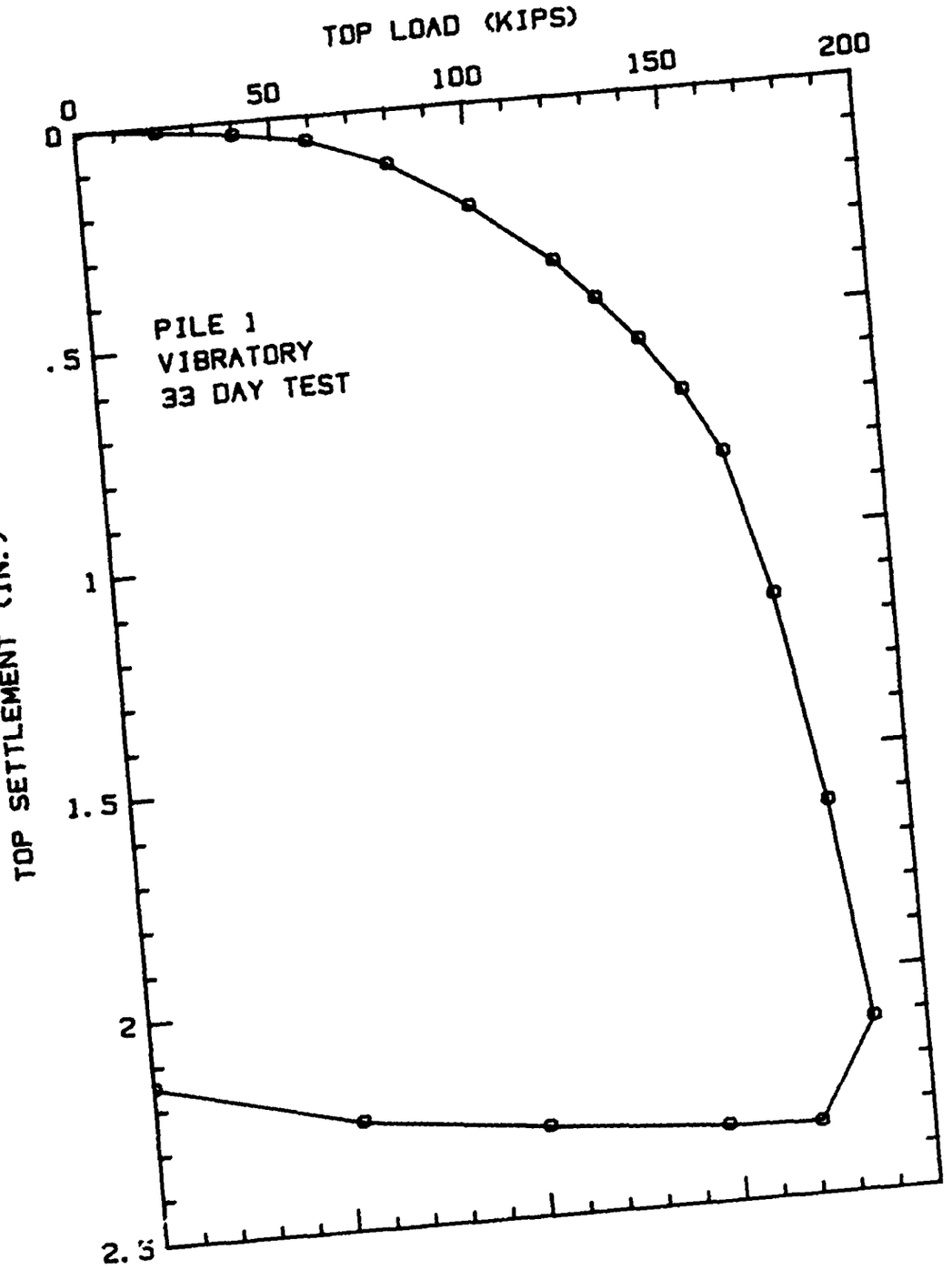

Figure 24. Load-Settlement Curve for Pile 1V

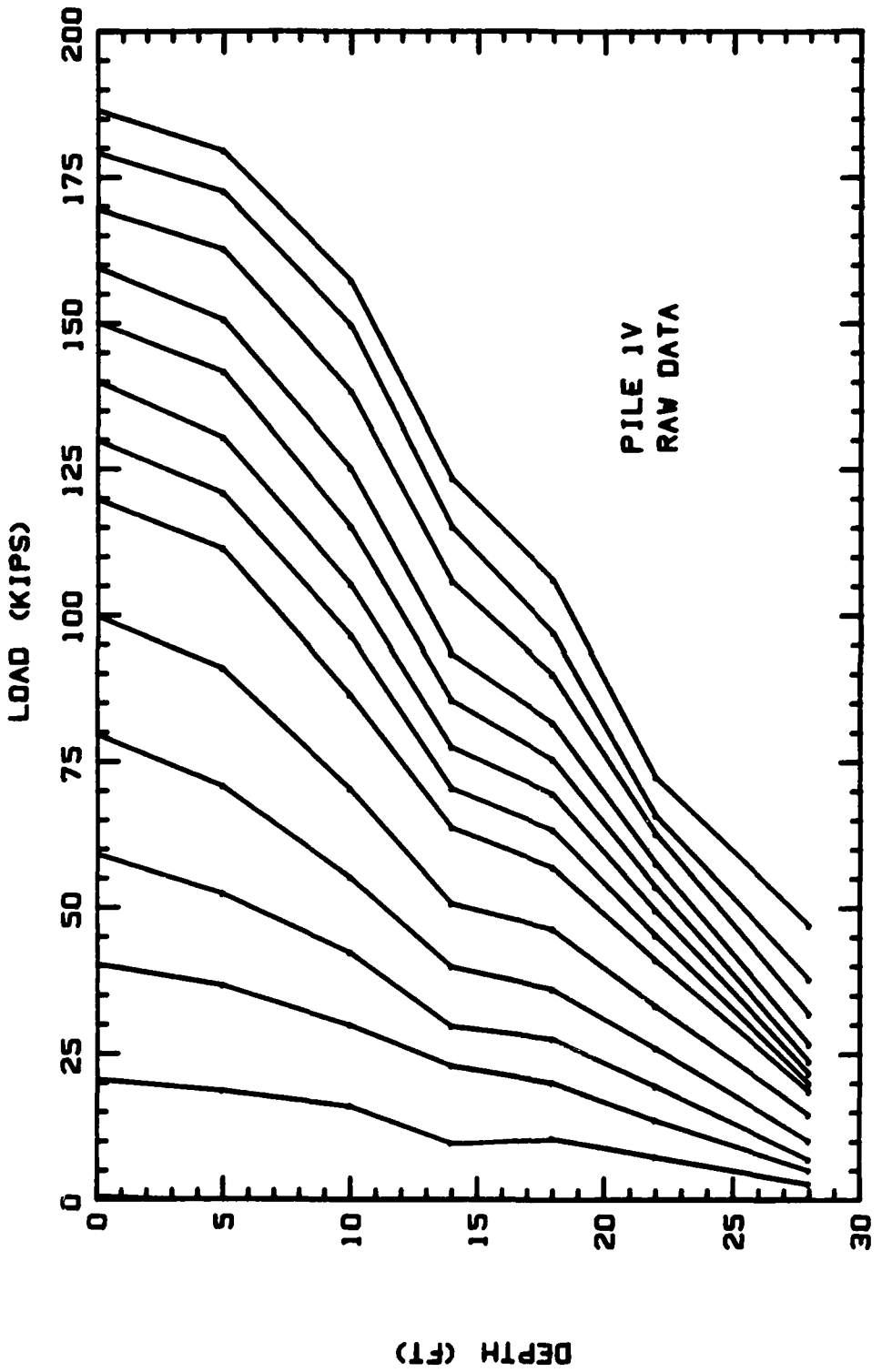

Figure 25. Raw Load Versus Depth Profiles for Pile 1V

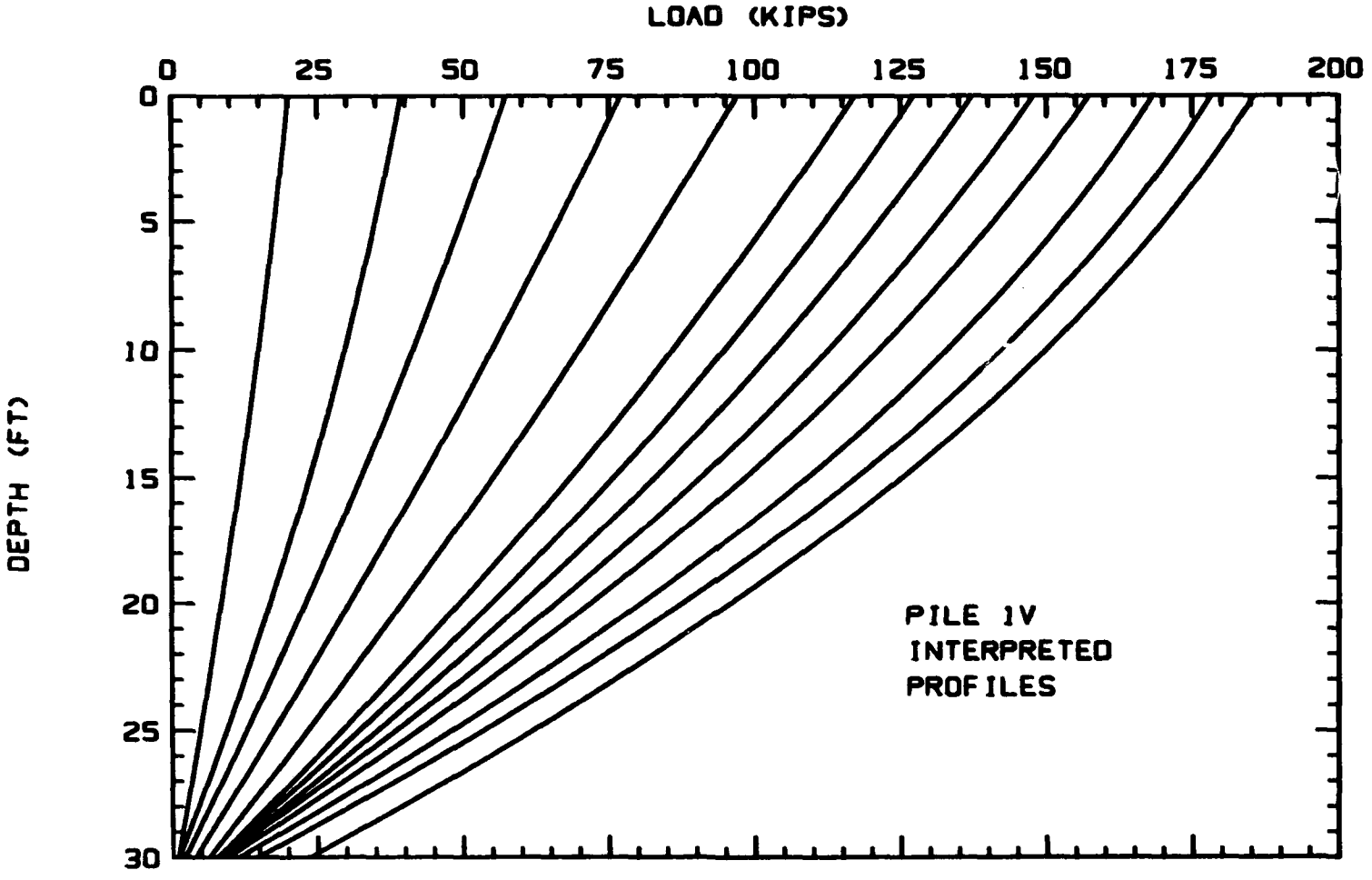

Figure 26. Interpreted Load Versus Depth Profiles for Pile 1V

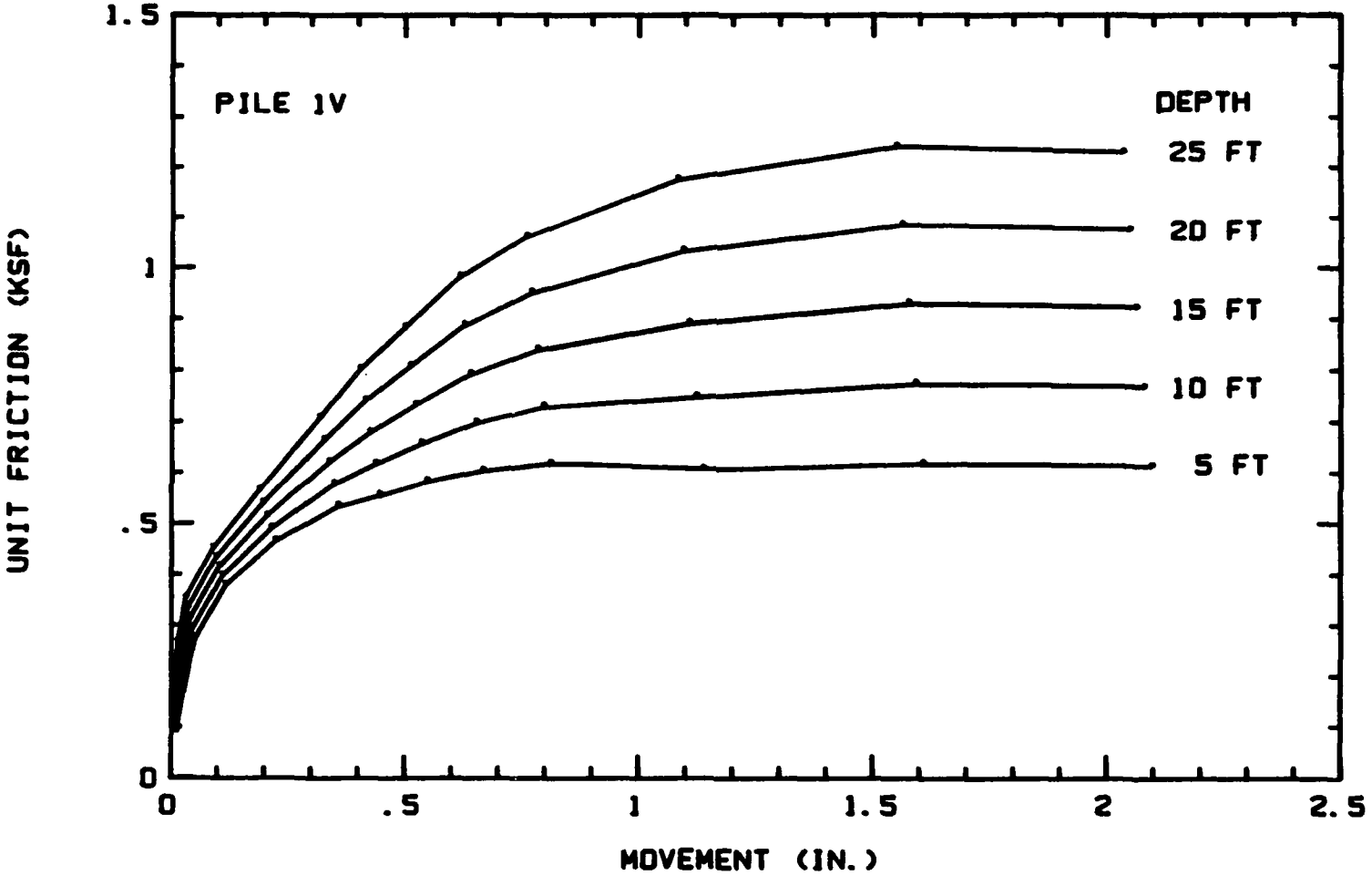

Figure 27. Friction Versus Movement Curves for Pile 1V

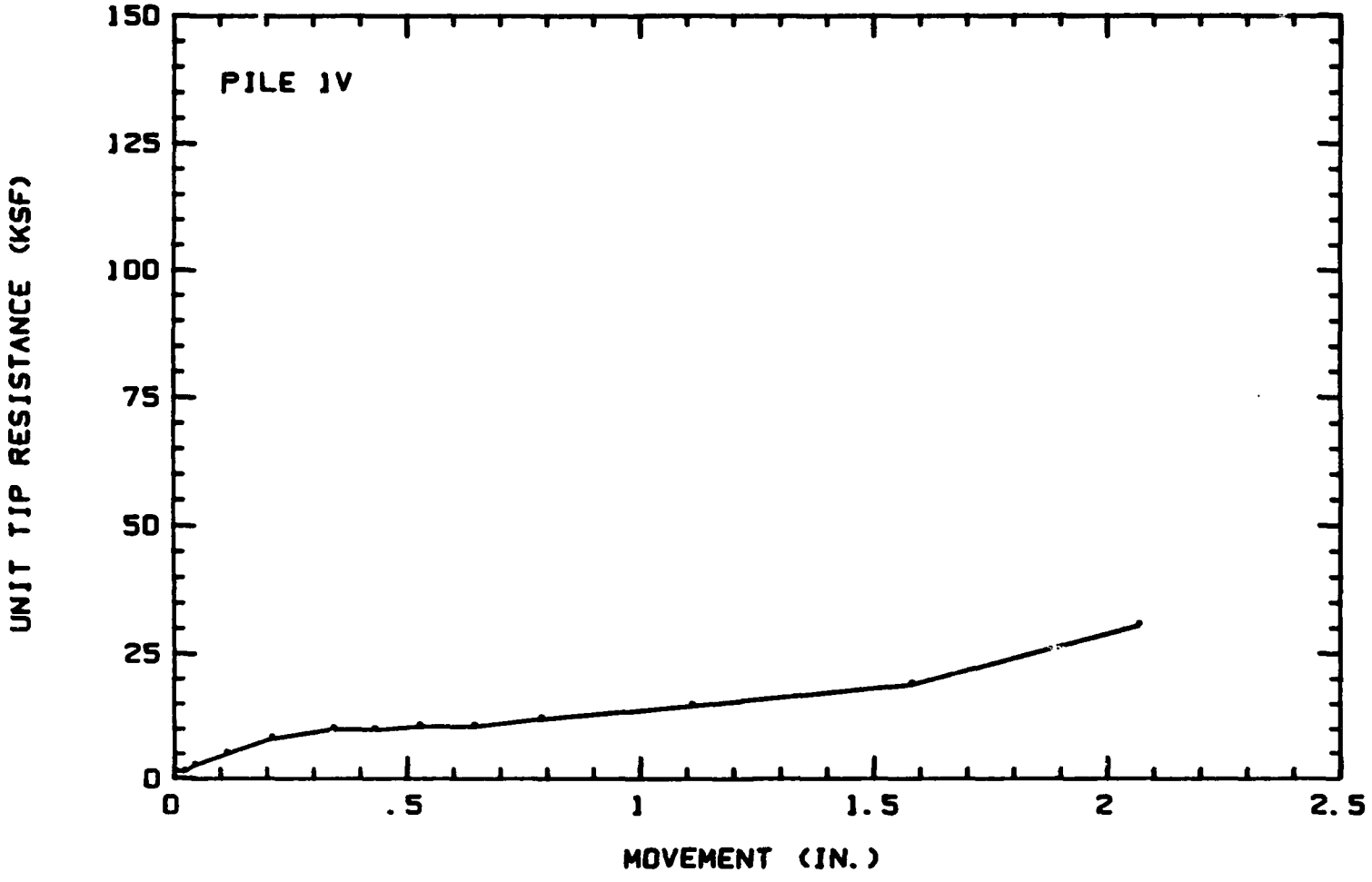

Figure 28. Point Resistance Versus Movement Curve for Pile 1V

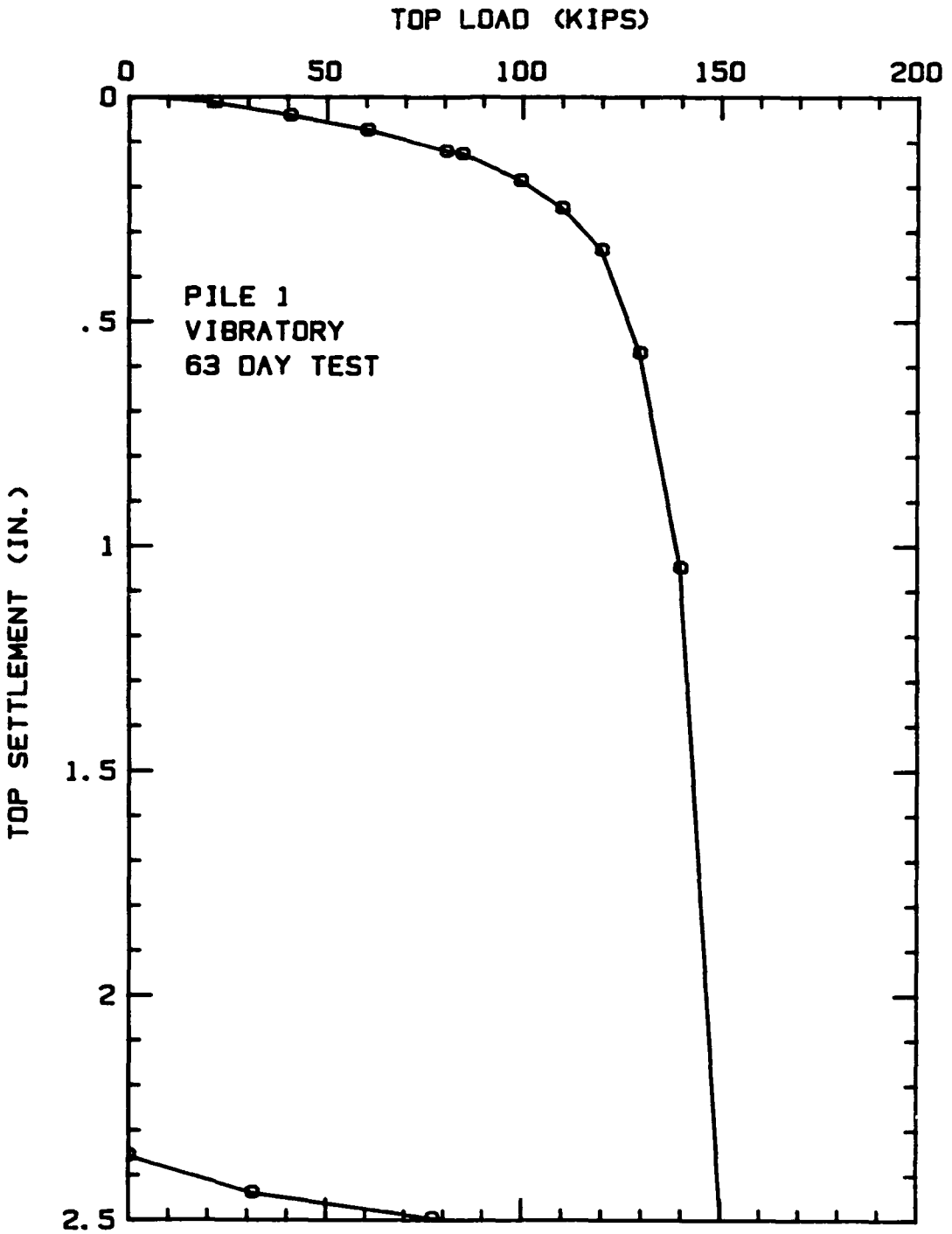

Figure 29. Load-Settlement Curve for Pile 1VR

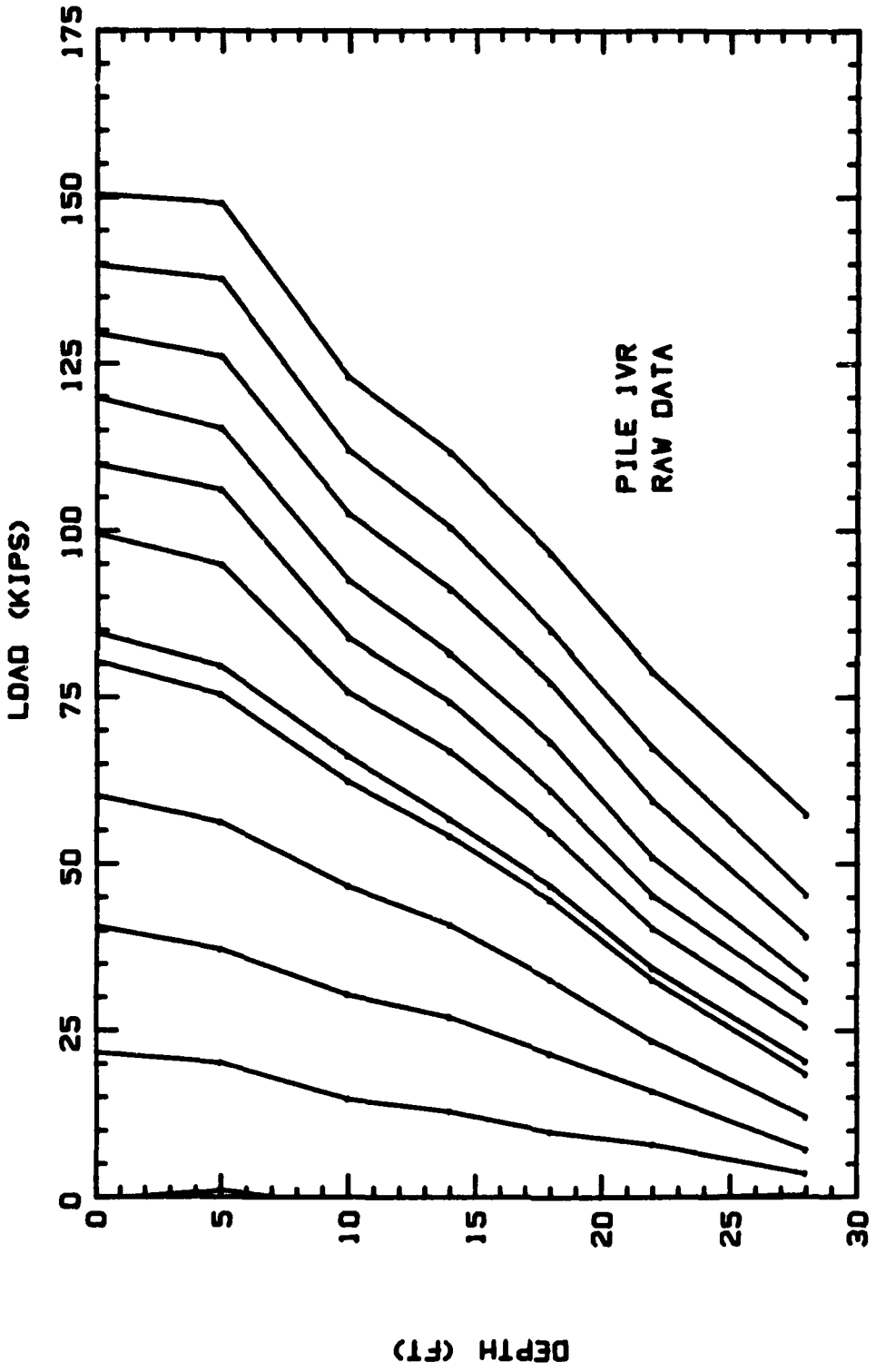

Figure 30. Raw Load Versus Depth Profiles for Pile 1VR

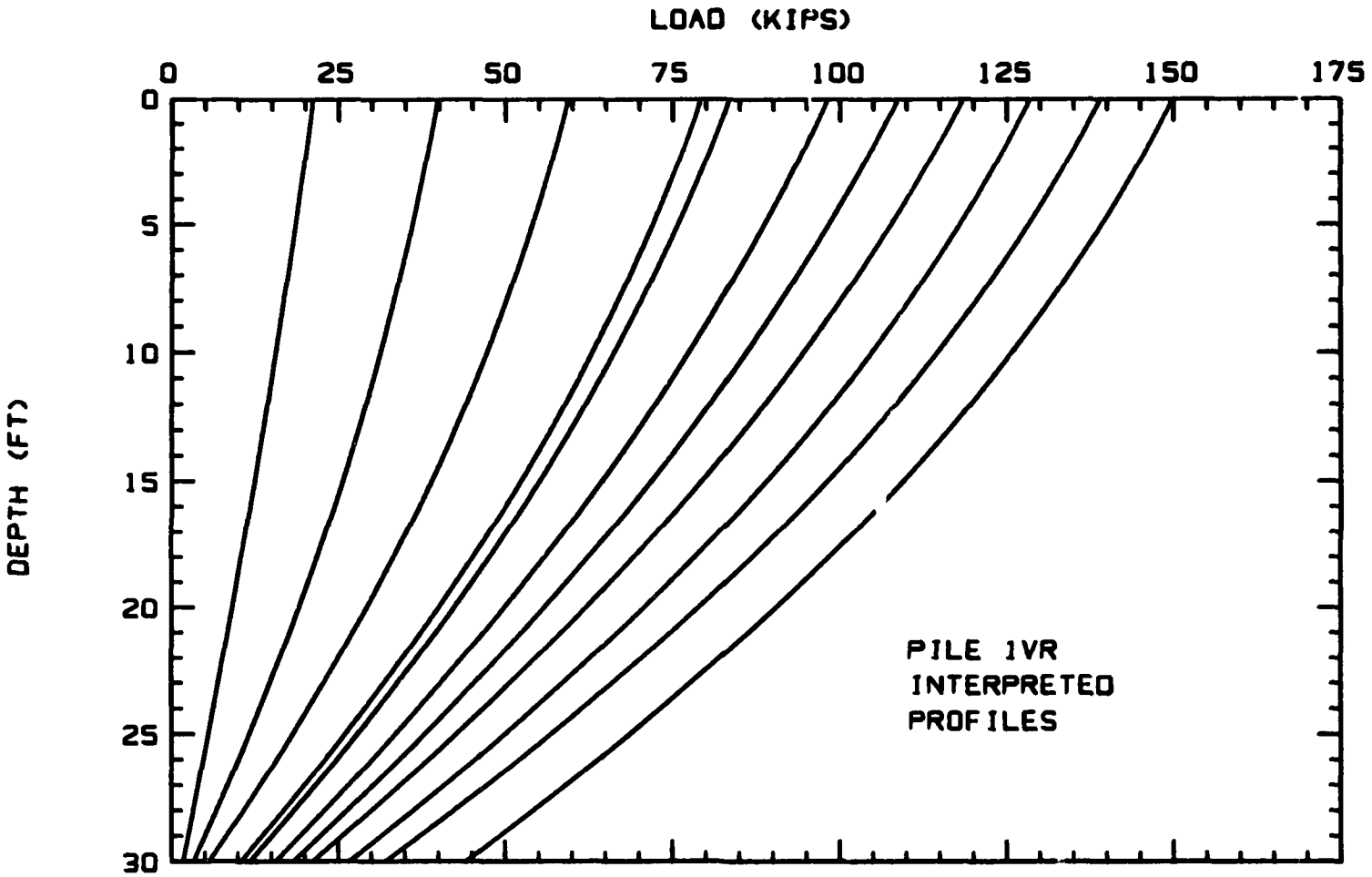

Figure 31. Interpreted Load Versus Depth Profiles for Pile 1VR

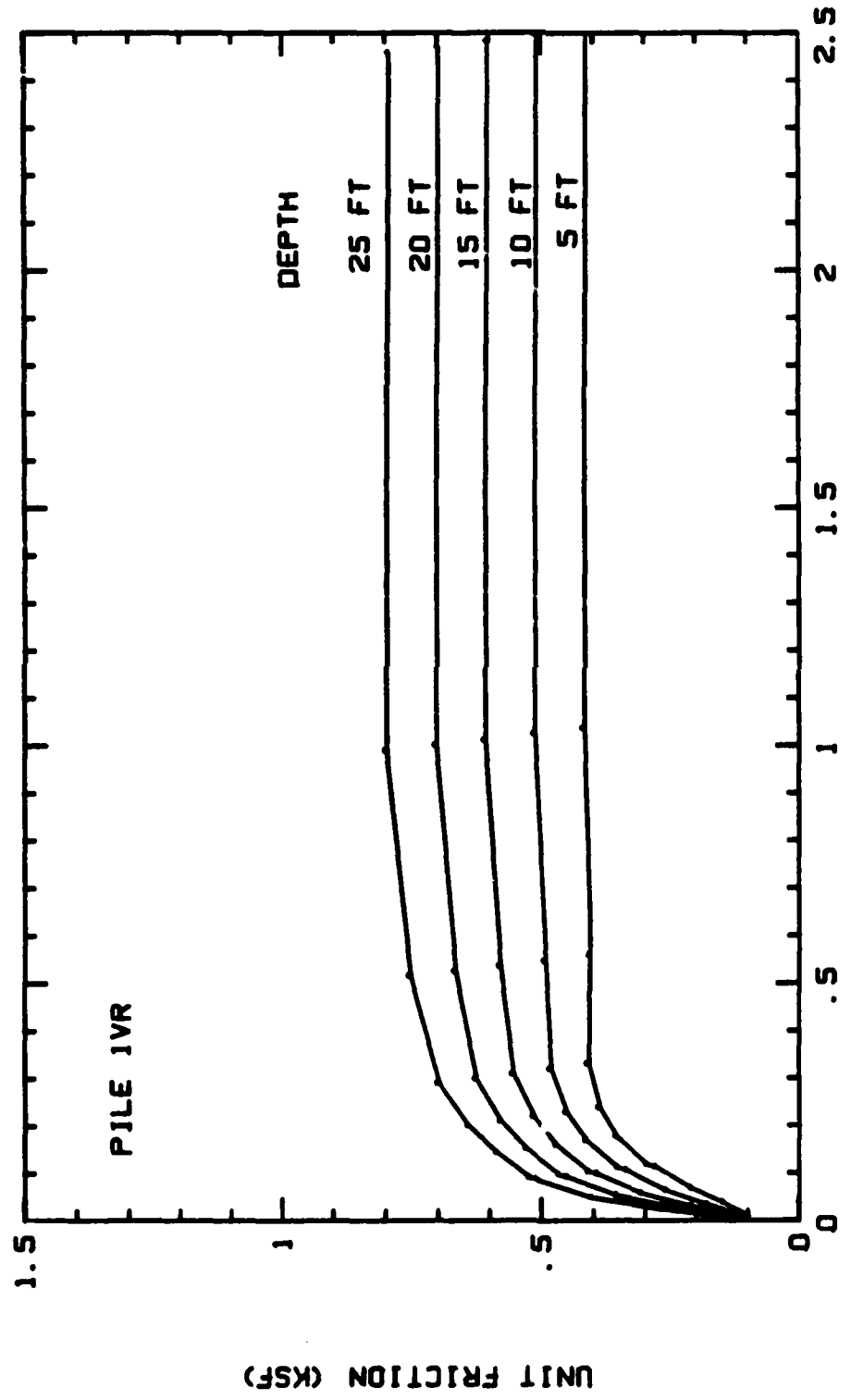

Figure 32. Friction Versus Movement Curves for Pile 1VR

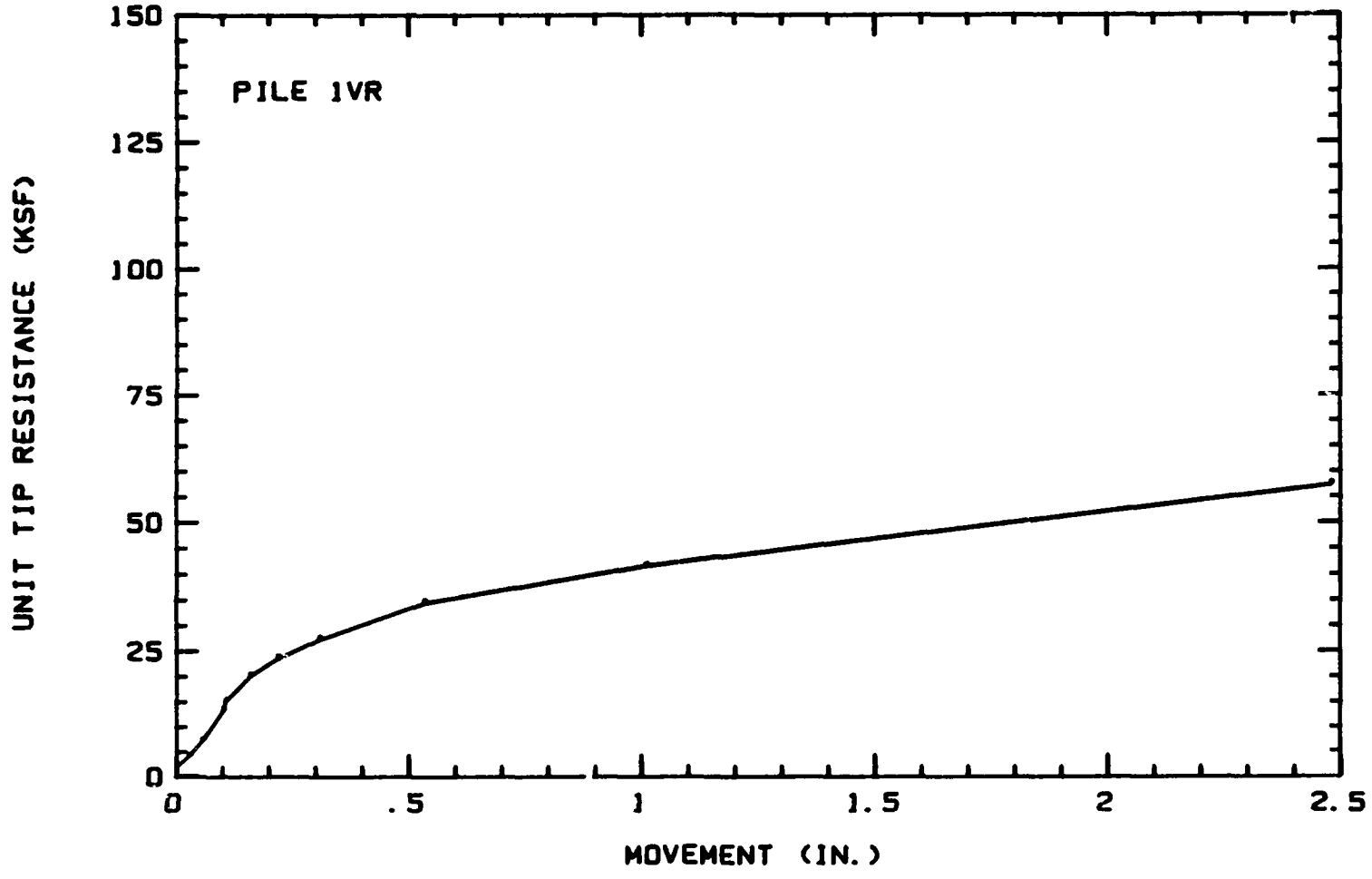

Figure 33. Point Resistance Versus Movement Curve for Pile 1VR

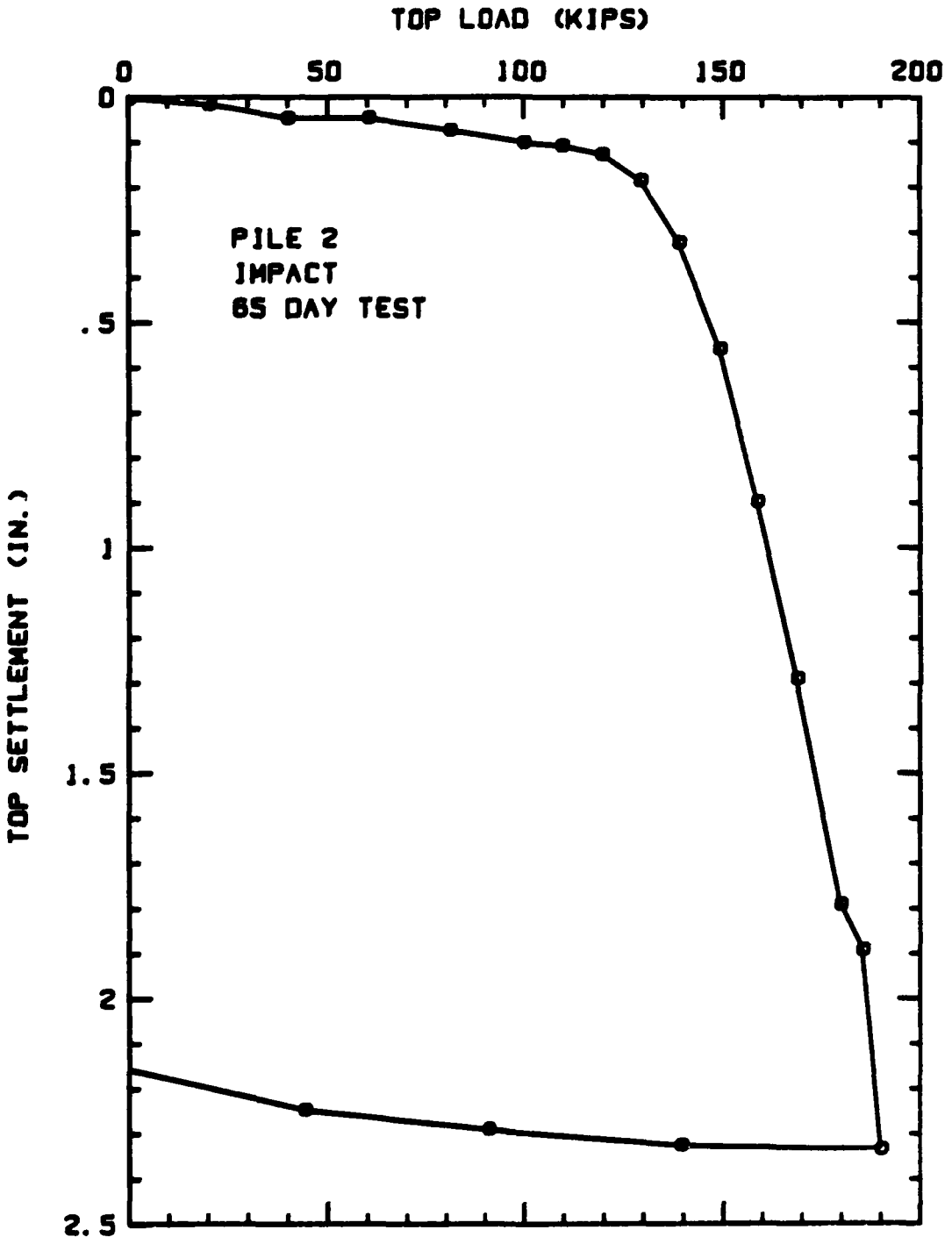

Figure 34. Load-Settlement Curve for Pile 2I

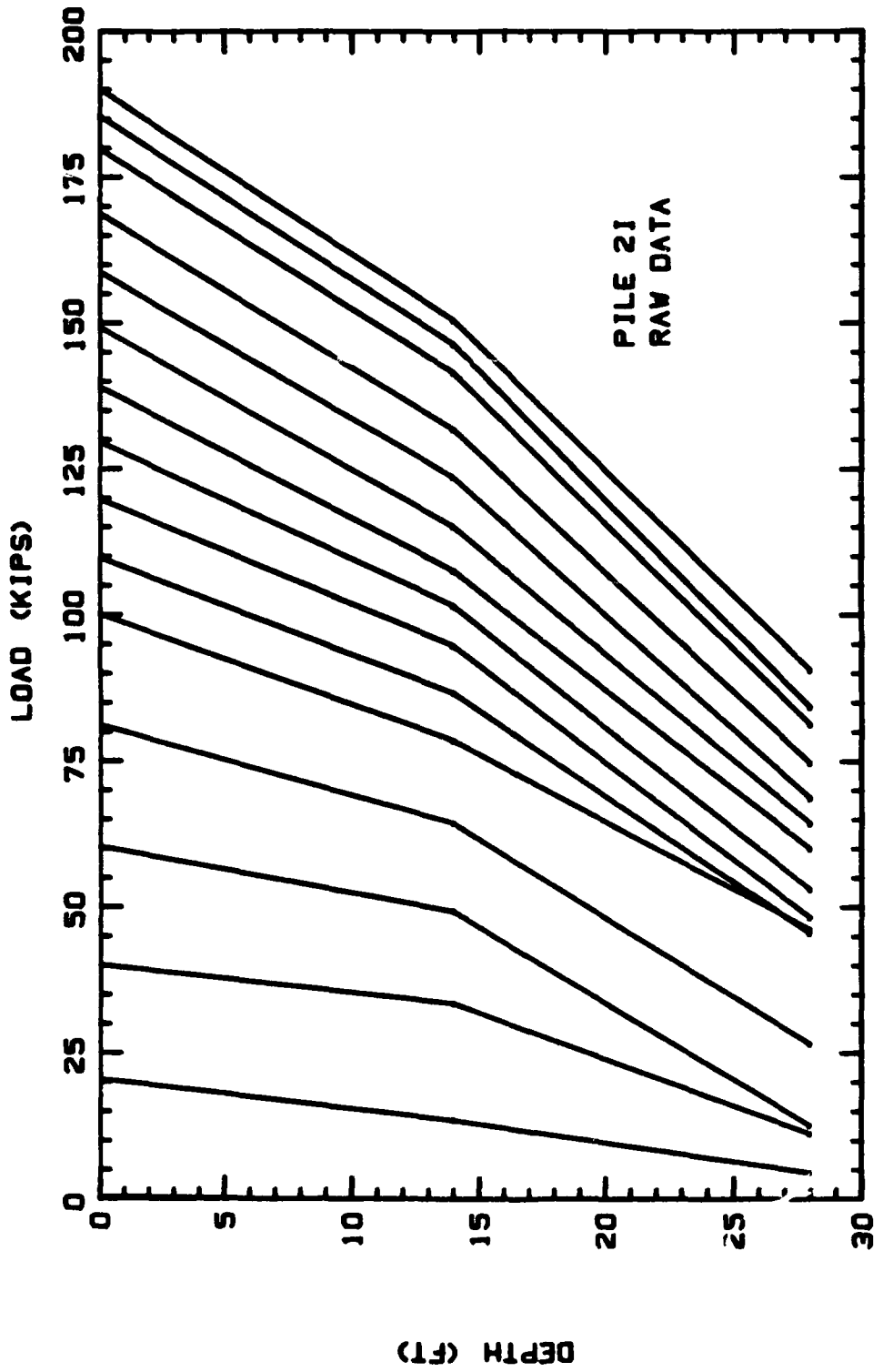

Figure 35. Raw Load Versus Depth Profiles for Pile 21

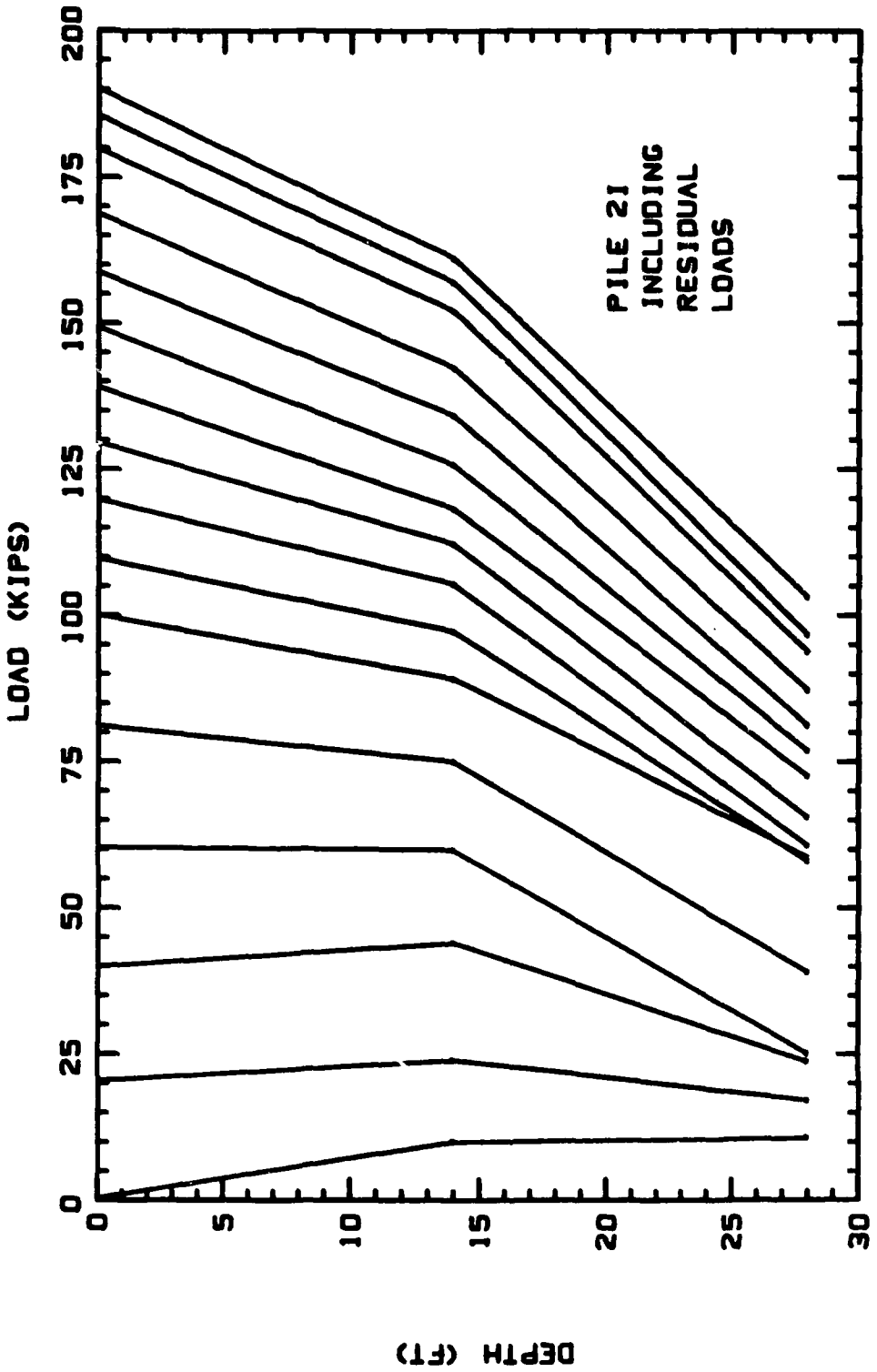

Figure 36. Corrected Load Versus Depth Profiles for Pile 2I

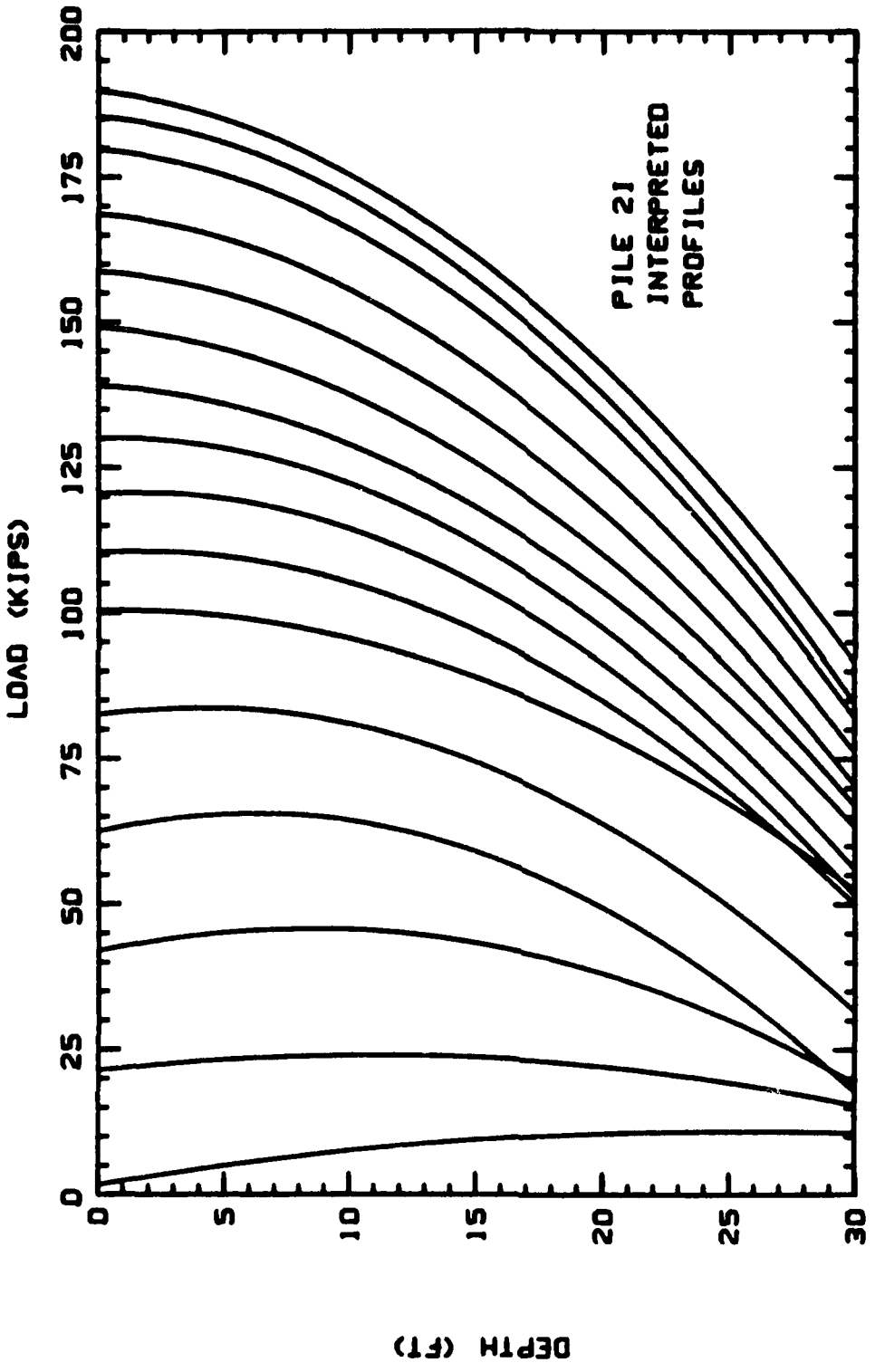

Figure 37. Interpreted Load Versus Depth Profiles for Pile 2I

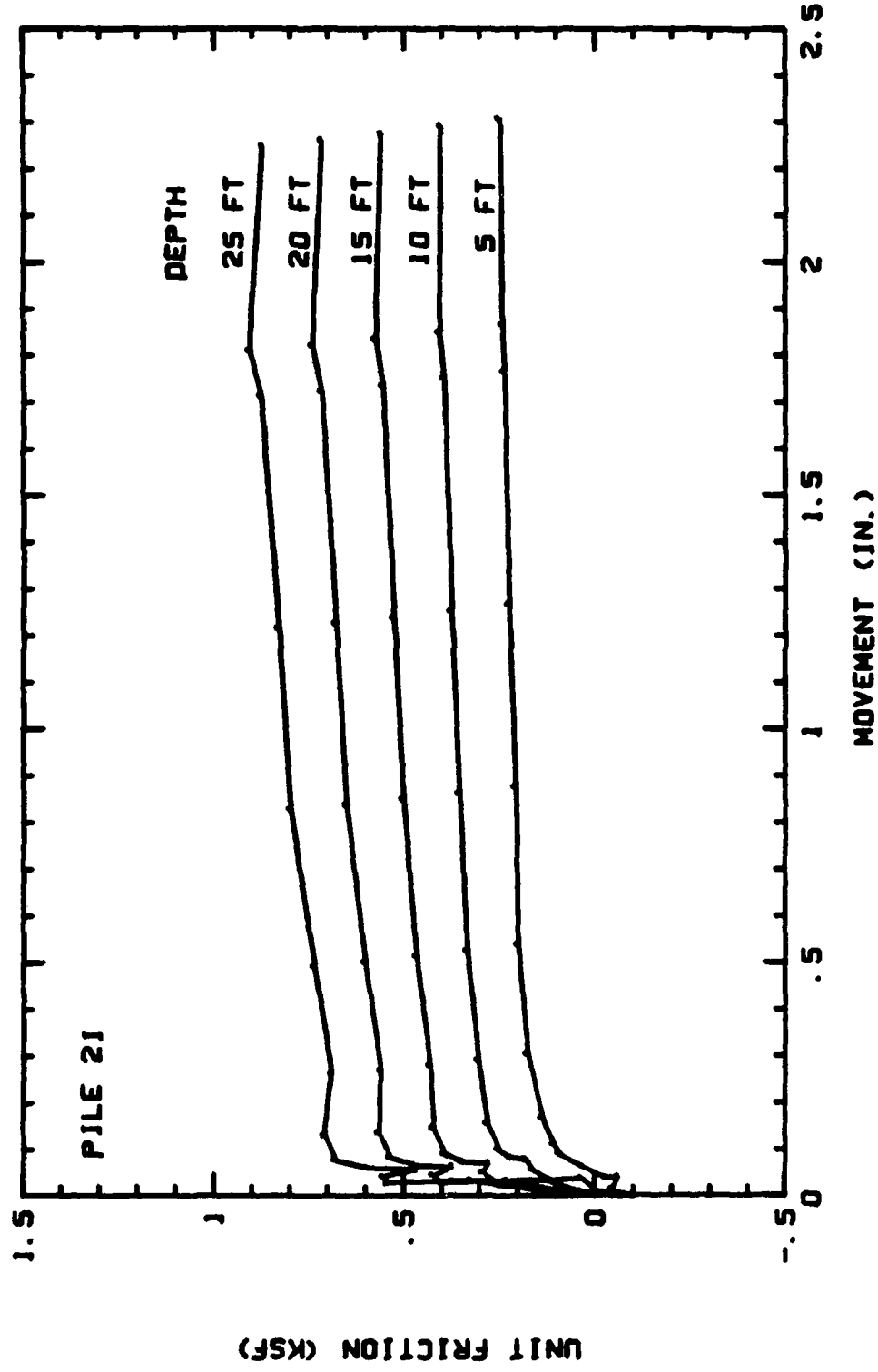

Figure 38. Friction Versus Movement Curves for Pile 21

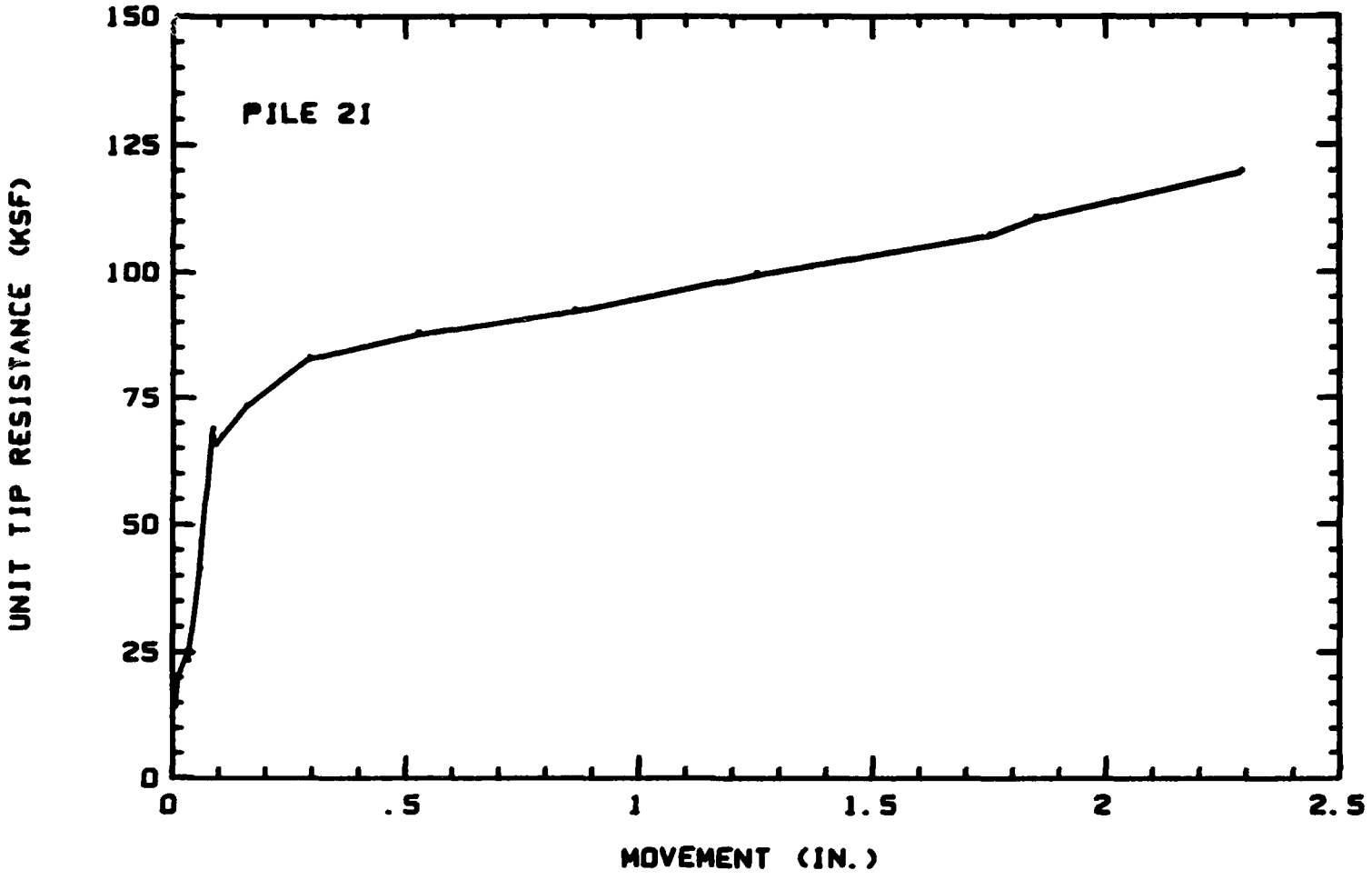

Figure 39. Point Resistance Versus Movement Curve for Pile 2I

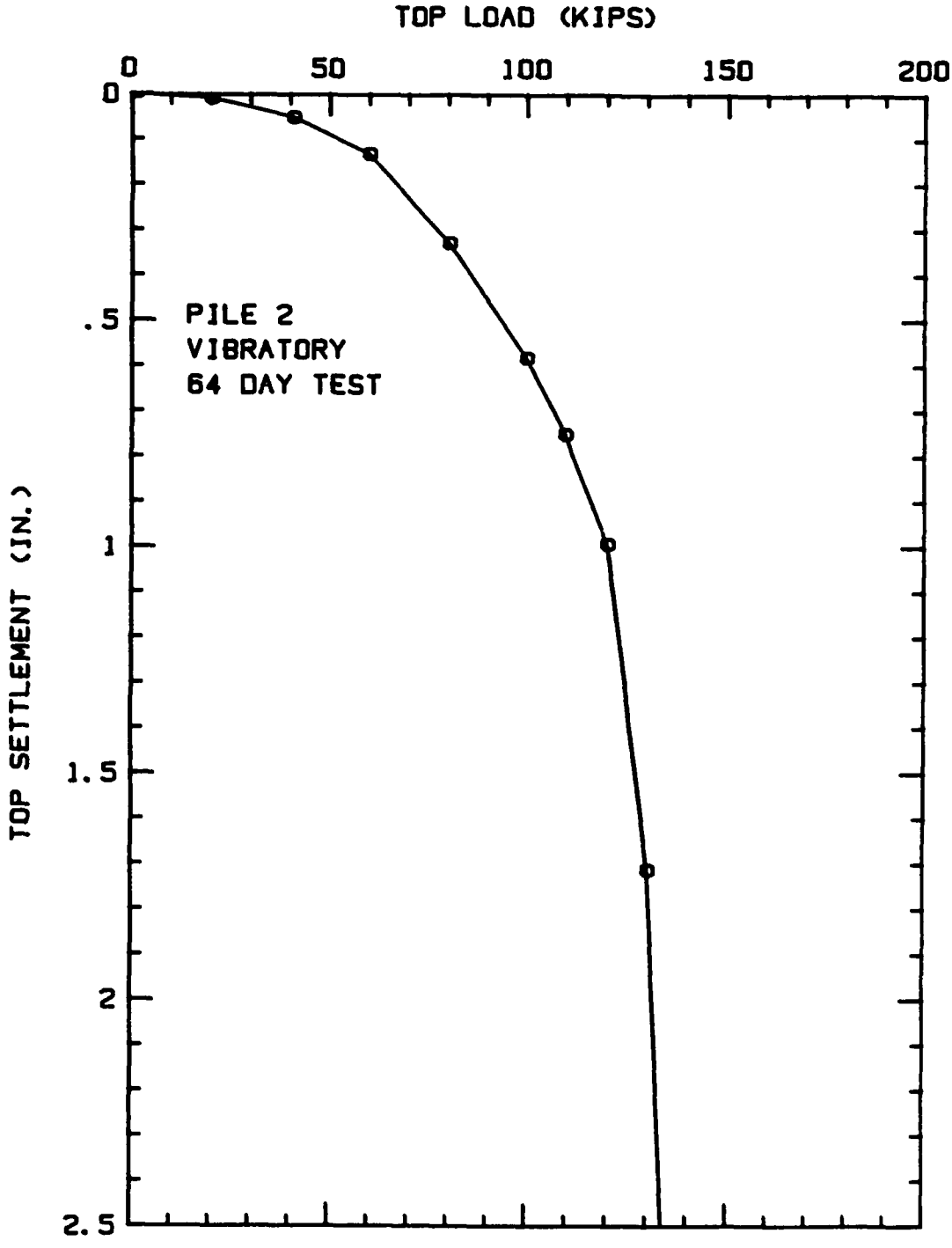

Figure 40. Load-Settlement Curve for Pile 2V

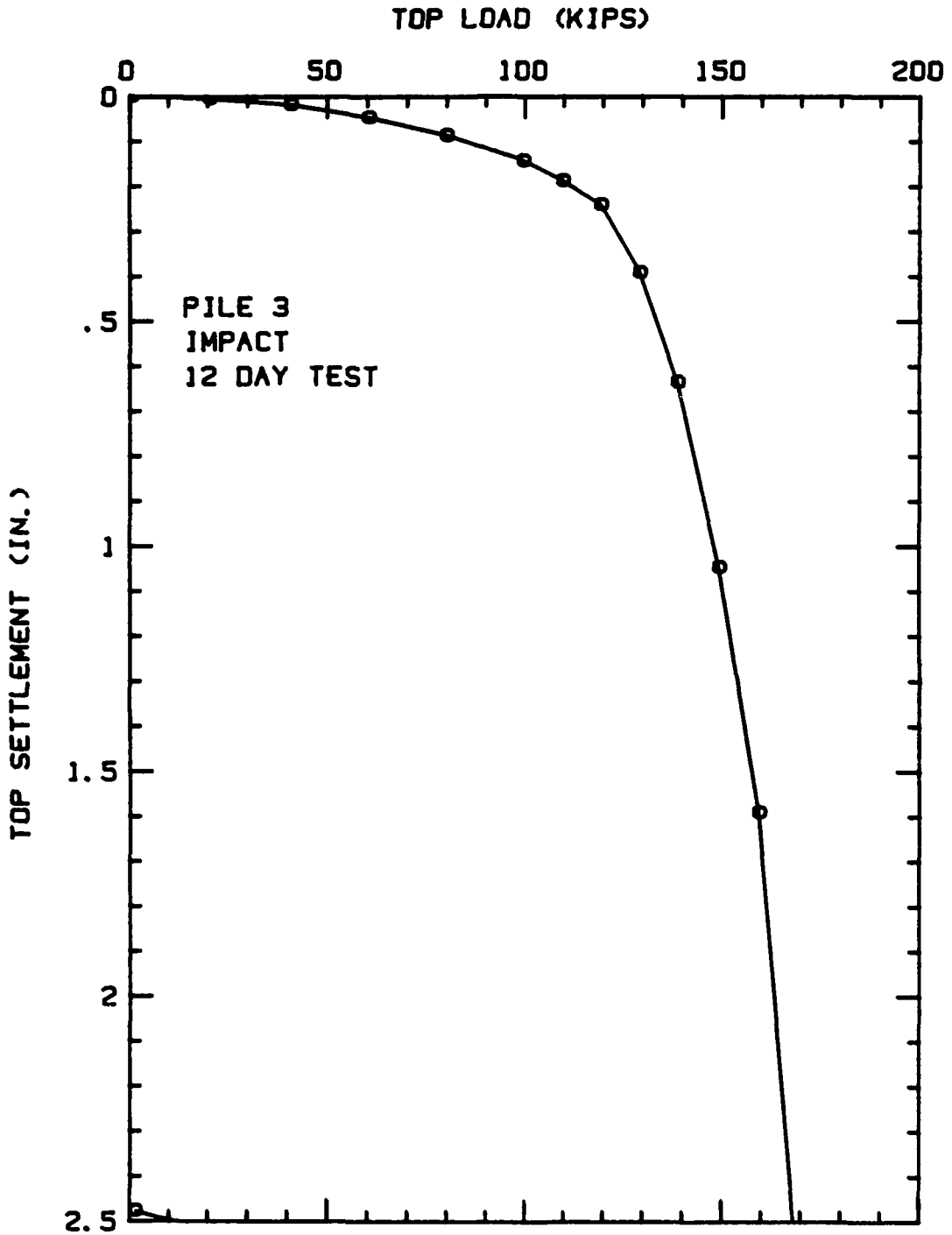

Figure 41. Load-Settlement Curve for Pile 3I

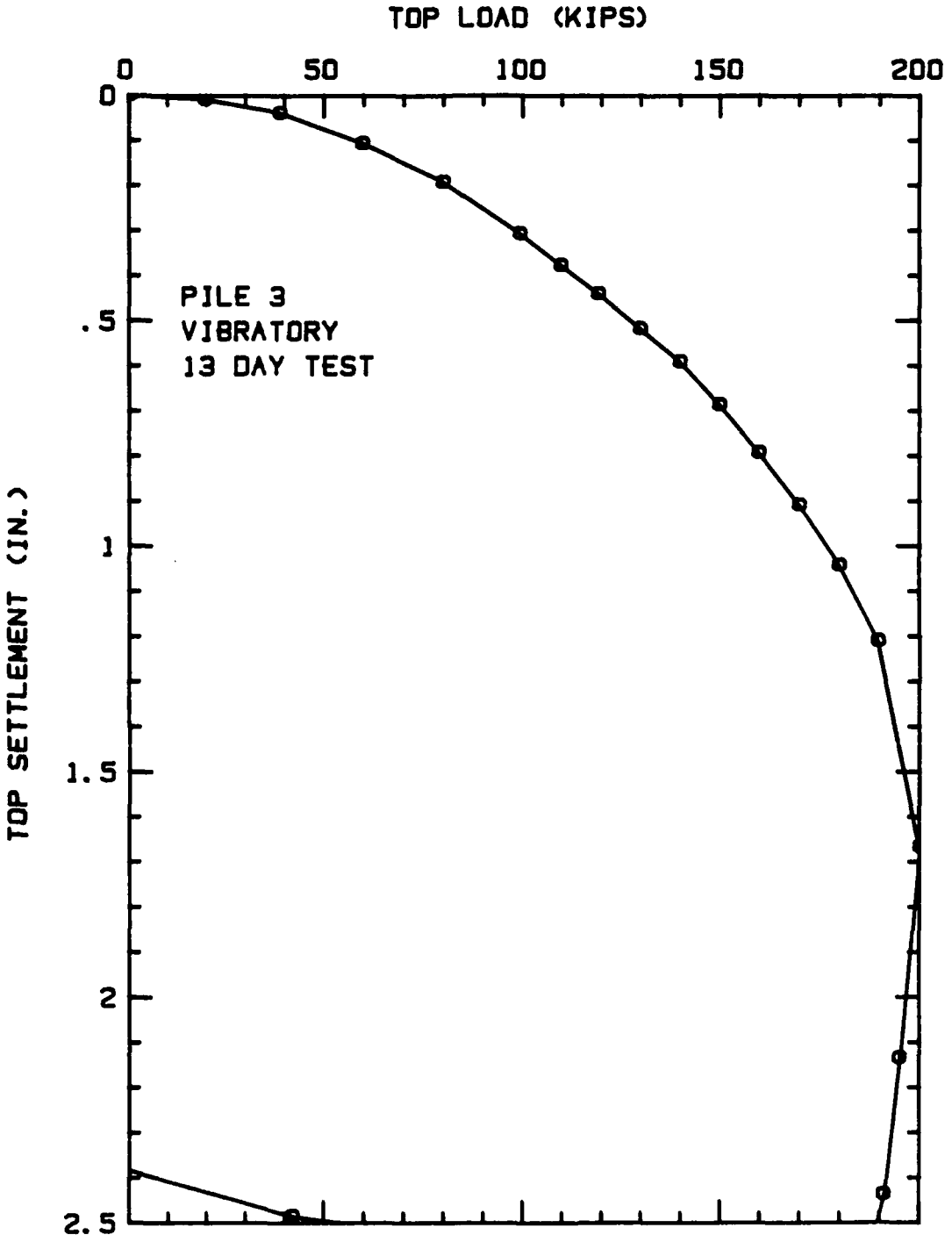

Figure 42. Load-Settlement Curve for Pile 3V

Pile Driving Analyzer Results

The pile driving analyzer (PDA) consists of the dynamic monitoring of strain gauges and accelerometers attached to the pile close to the top. The strain measurements are used to obtain force measurements as a function of time, and the accelerometer measurements are integrated to obtain velocity versus time. From these two measurements various parameters may be calculated, including the maximum energy delivered to the pile and the static resistance of the pile by the CASE method (Rausche et al., 1985). This static resistance represents the PDA capacity prediction.

Pile driving analyzer measurements were made on pile 1 (driven with the impact hammer) for both initial driving and for restrike after the load tests were performed, and on piles 1 and 2 (driven with the vibratory hammer) for restrike after the load tests were performed. The results are presented in Table 4.

Table 4. Pile Driving Analyzer Results
(from Holloway, 1987)

Pile	Blowcount	Maximum Force (kips)	Maximum Energy (kip-ft)	Estimated Capacity* (kips)
1I**	12/12 in.	340-510	5-15	140-165
1I***	6/6 in.	350-505	10-17	145-200
1V***	7/6 in.	300-415	4-13	120-140
2V***	14/12 in.	355-520	5-11	125-150

* Case method capacity assumes a damping constant J=0.25
** Initial driving
*** Restrike

DISCUSSION OF THE RESULTS

Top Load-Settlement Curves

The top load-settlement curves for the eight load tests are shown together in Figure 43. Two main observations can be made. First, in all cases the vibratory driven piles have a lower initial stiffness than the impact driven piles. Second, the impact driven piles show more consistent response between piles than the vibratory driven piles.

In an effort to quantify these observations four measurements have been made from the load-settlement curves. First, the ultimate load has been defined as the load corresponding to a settlement of one-tenth of the equivalent pile diameter plus the elastic compression of the pile under that load as if it acted as a free-standing column. This line has been drawn on Figure 43. Second, the load at a settlement of 0.25 in has been obtained from the load-settlement curves. Third, the settlement at one-half the defined ultimate load has been obtained. Fourth, the piles' stiffness response has been calculated as one-half the defined ultimate load divided by the settlement occurring at that load. These four items are tabulated in Table 5 for the eight load tests.

Table 5 shows that there is only one percent difference in the average ultimate load between the impact driven piles and the vibratory driven piles. However, the coefficient of variation of the ultimate loads for the vibratory driven piles is 4.3 times higher than that of the impact driven piles.

The second column of Table 5 shows that at a settlement of 0.25 in the impact driven piles carry 33 percent more load than the vibratory driven piles. The coefficient of variation of this load for the vibra-

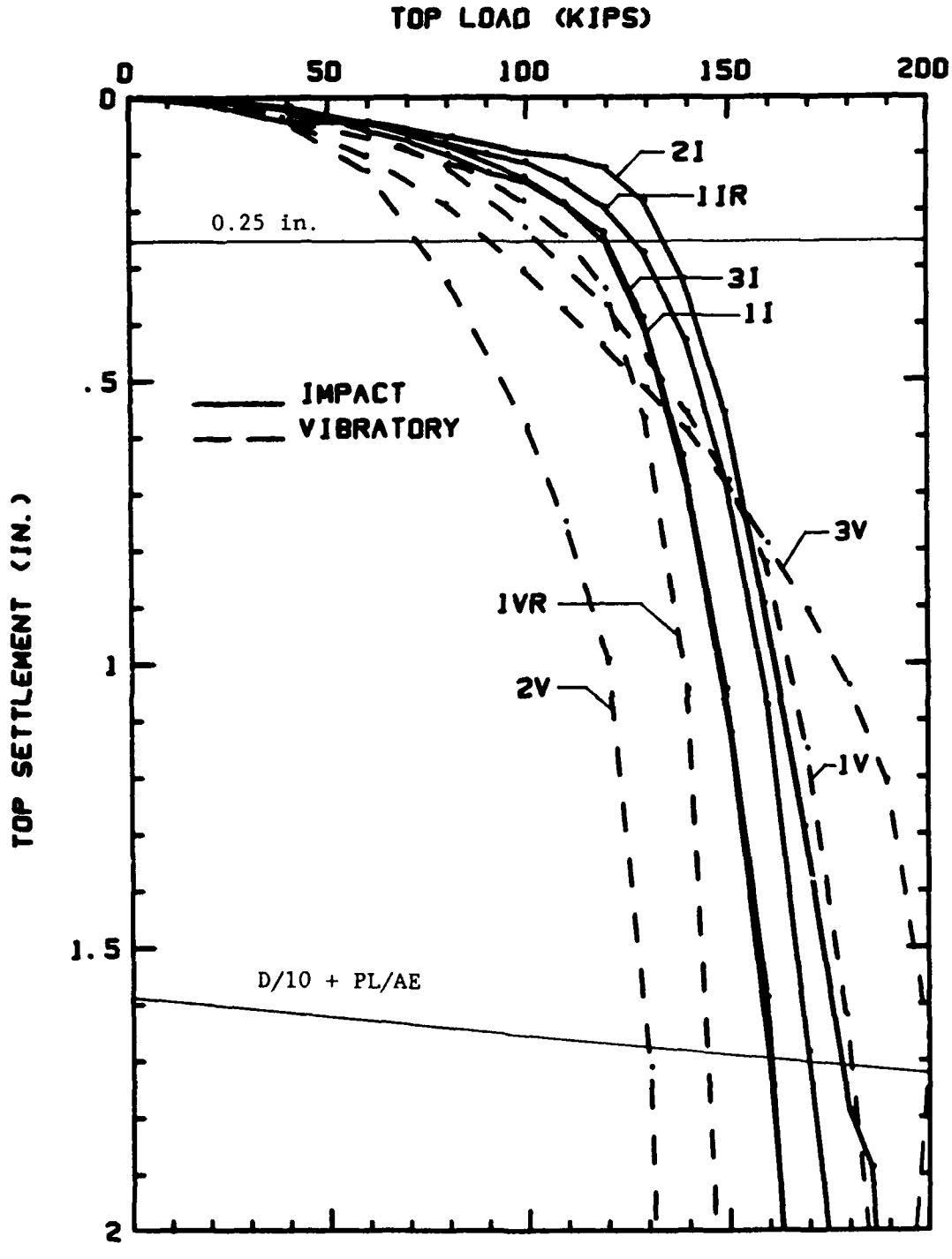

Figure 43. Comparison of Load-Settlement Curves

Table 5. Analysis of Pile Test Results

Pile	Load at D/10 + PL/AE (kips)	Load at 0.25 in. (kips)	Settlement at Qult/2 (in)	Initial Stiffness (kips/in)
1I	160	120	0.104	769
1IR	170	126	0.094	904
2I	175	131	0.088	994
3I	160	120	0.088	909
Average	166	124	0.094	894
Standard Deviation	7.5	5.3	0.0075	93
Coefficient of Variation	0.045	0.043	0.081	0.104
1V	180	102	0.181	497
1VR	145	110	0.103	704
2V	130	71	0.184	353
3V	200	90	0.313	319
Average	164	93	0.195	468
Standard Deviation	32	17	0.087	175
Coefficient of Variation	0.195	0.182	0.446	0.374
Impact / Vibratory	1.01	1.33	0.48	1.91

tory driven piles is 4.2 times higher than that of the impact driven piles.

The settlement at one-half the ultimate load for the vibratory driven piles is over two times larger than that of the impact driven piles, and the coefficient of variation is 5.5 times larger.

The initial stiffness response of the pile, defined as one-half the ultimate load divided by the settlement at that load, for the impact driven piles is 1.91 times that of the vibratory driven piles. The coefficient of variation of this stiffness for the vibratory driven piles is 3.6 times that of the impact driven piles.

Load Distribution

The load distribution of the vibratory driven piles differs greatly from that of the impact driven piles. By comparing Figures 15, 21, 26, 31, and 37 it can be seen that at maximum load the impact driven piles carry approximately 51% of the load in point resistance, whereas the vibratory driven pile carries only 13% of the load in point resistance. The reload test on the vibratory driven pile (Figure 31) shows that the point resistance has increased to 29% of the total load. This indicates that the difference in the driving process causes a different soil reaction, but the difference becomes less upon repeated loading.

The unit friction profiles at maximum loading are shown in Figure 44 for the five instrumented pile tests. Again in can be seen that there is a definite difference in soil reaction between the impact driven and vibratory driven piles; and that the difference becomes less pronounced upon repeated loading.

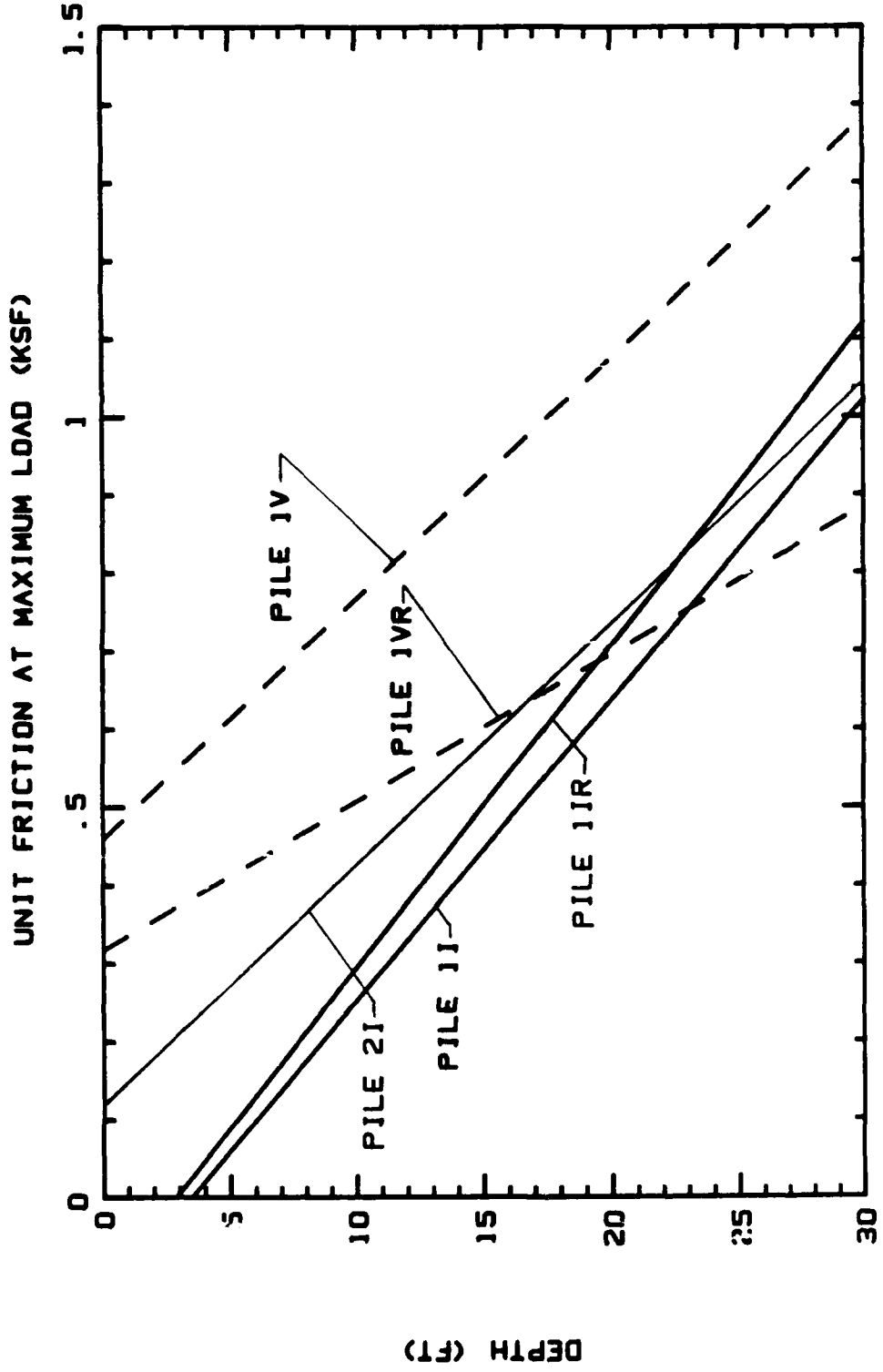

Figure 44. Friction Versus Depth Profiles

Load Transfer

The H-pile presents a problem when computing unit tip resistance and unit friction values: What is the failure surface? One possible assumption is that the pile fails along a rectangle which encloses the H-pile, with a soil plug forming between the flanges. Another possibility is that the pile fails along the soil-pile interface, with no soil plug forming. Previous research has shown that a better assumption may be that the failure surface is in between the previous two assumptions with a soil plug filling half the area between the flanges (Ng et al., 1988). For the HP14x73 piles used in this study this assumption gives the following properties: Perimeter = 70.47 in, Tip area = 109.8 in^2. This assumption is used for all further analyses.

Figure 45 shows the unit tip resistance versus tip movement curves for the five instrumented piles. Figure 46 shows the same curves with the tip resistance normalized by dividing by the maximum tip resistance. These two figures show a fundamentally different reaction between the vibratory driven piles and the impact driven piles: The tip resistance of the vibratory driven piles is much lower than that of the impact driven piles, and the slope of the curve is different. However, the difference in shape almost vanishes upon reloading.

The shape of the tip resistance curve of the initial loading of the vibratory driven pile suggests that the sand immediately under the pile point is initially loose but densifies as the pile is loaded. Indeed, at higher loads the tip resistance begins to increase at a faster rate, rather than reaching a limiting value as the other tests show. By comparing the curves for Pile 1I and 1IR, it can be seen that the impact

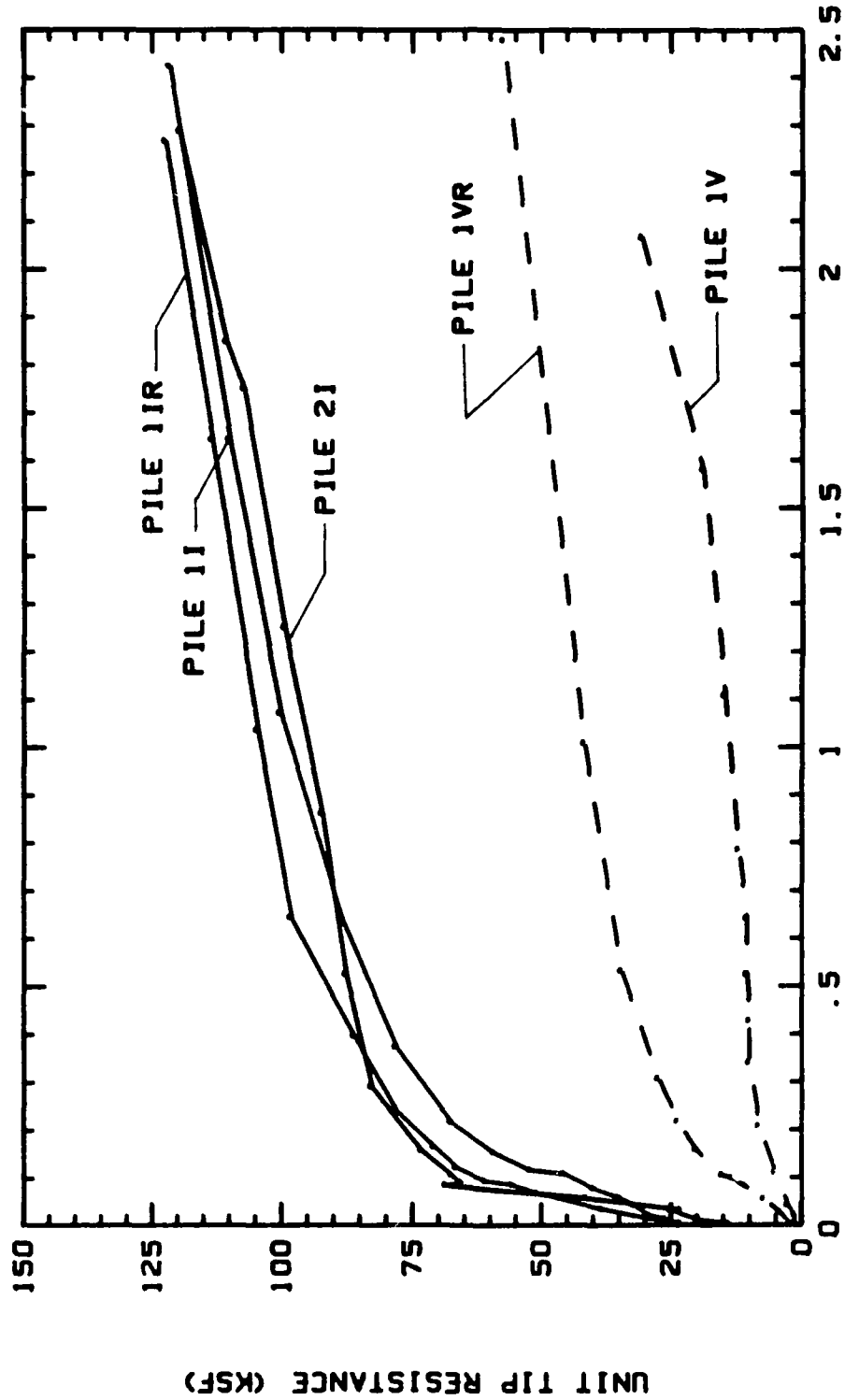

Figure 45. Comparison of Point Load Transfer Curves

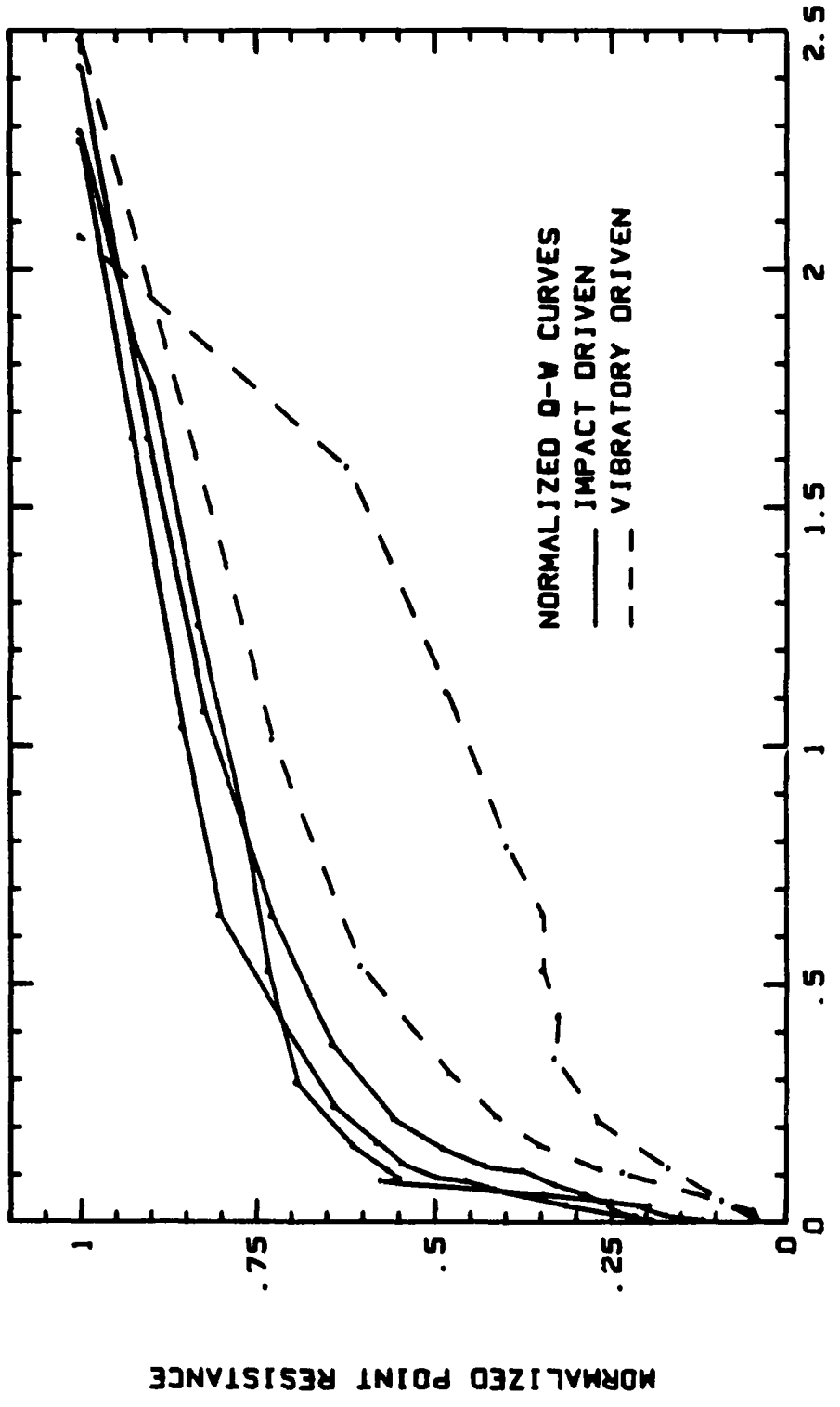

Figure 46. Normalized Point Load Transfer Curves

driven piles do not undergo such a change in behavior between initial loading and reloading.

Figures 47 and 48 show the normalized friction movement curves for the impact driven piles and vibratory driven piles, respectively. Figure 47 shows again that the impact driven piles are very consistent in their response and that no change in behavior occurs between initial loading and reloading. However, Figure 48 shows that the vibratory driven pile exhibits a great change in behavior between initial loading and reloading. The five curves for the initial loading have a much softer initial response than the reloading curves. Also the initial loading curves become softer as the depth increases, whereas the reload curves become stiffer as the depth increases. The reloading curves also exhibit a pattern which matches the impact driven piles very well.

Effect of Time

Piles 1I and 1V were tested about 31 days after driving and then retested about 65 days after driving. The plots of ultimate load versus time for two criteria are shown in Figures 49 and 50. The trend given by those two figures does not allow to conclude that there is an increase in capacity versus time. Indeed Figure 49 shows an increase in stiffness but Figure 50 shows a decrease in capacity for the vibratory driven piles; for the impact driven piles Figure 49 shows an increase while Figure 50 shows a slight increase. At Lock and Dam 26 the capacity obtained in the load test was 67% higher than the capacity predicted by the wave equation method on the average. This can be explained by a 67% average gain in capacity of the piles between driving and load testing of the piles (1 week). Note that the sand at Lock and

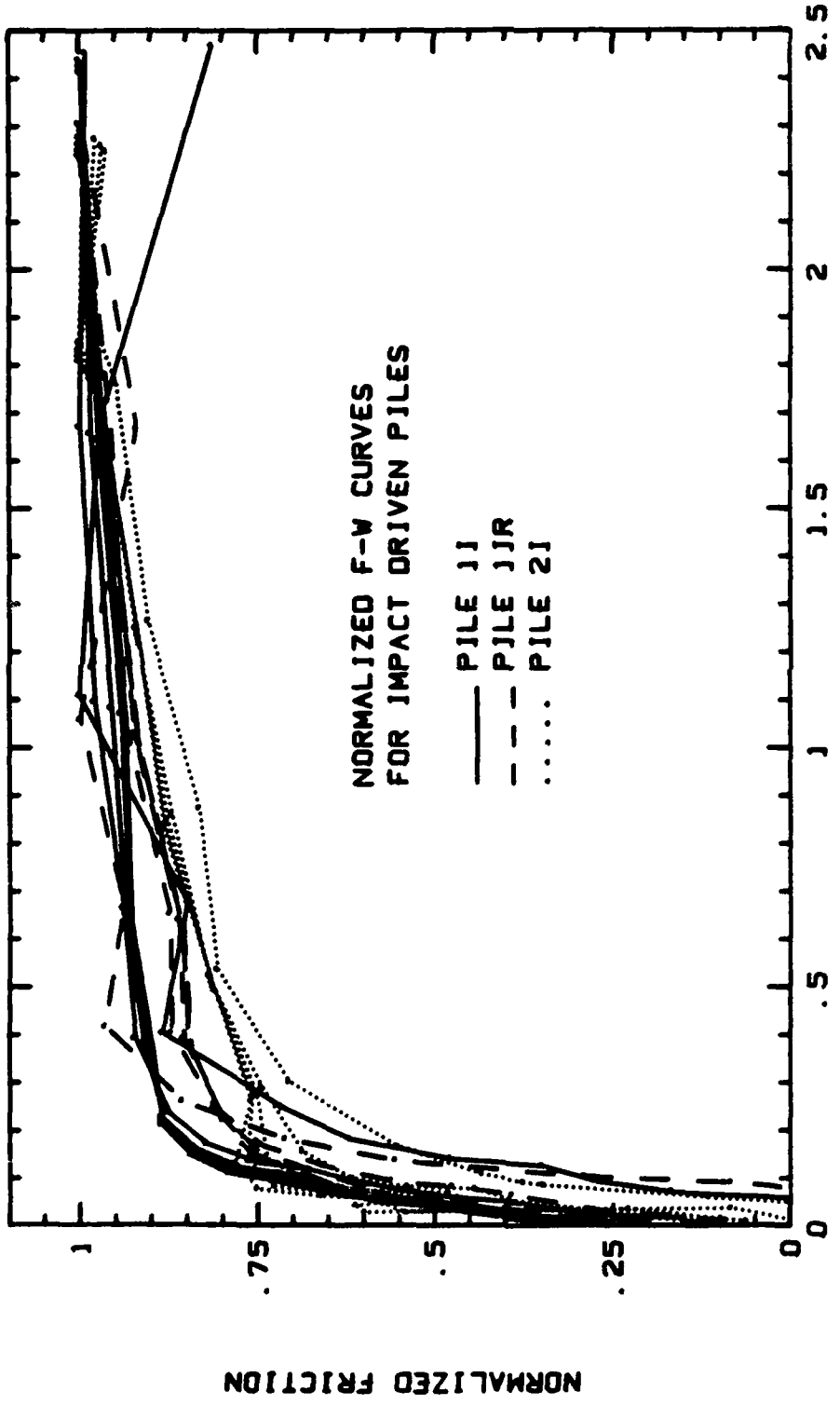

Figure 47. Normalized Friction Transfer Curves for Impact Driven Piles

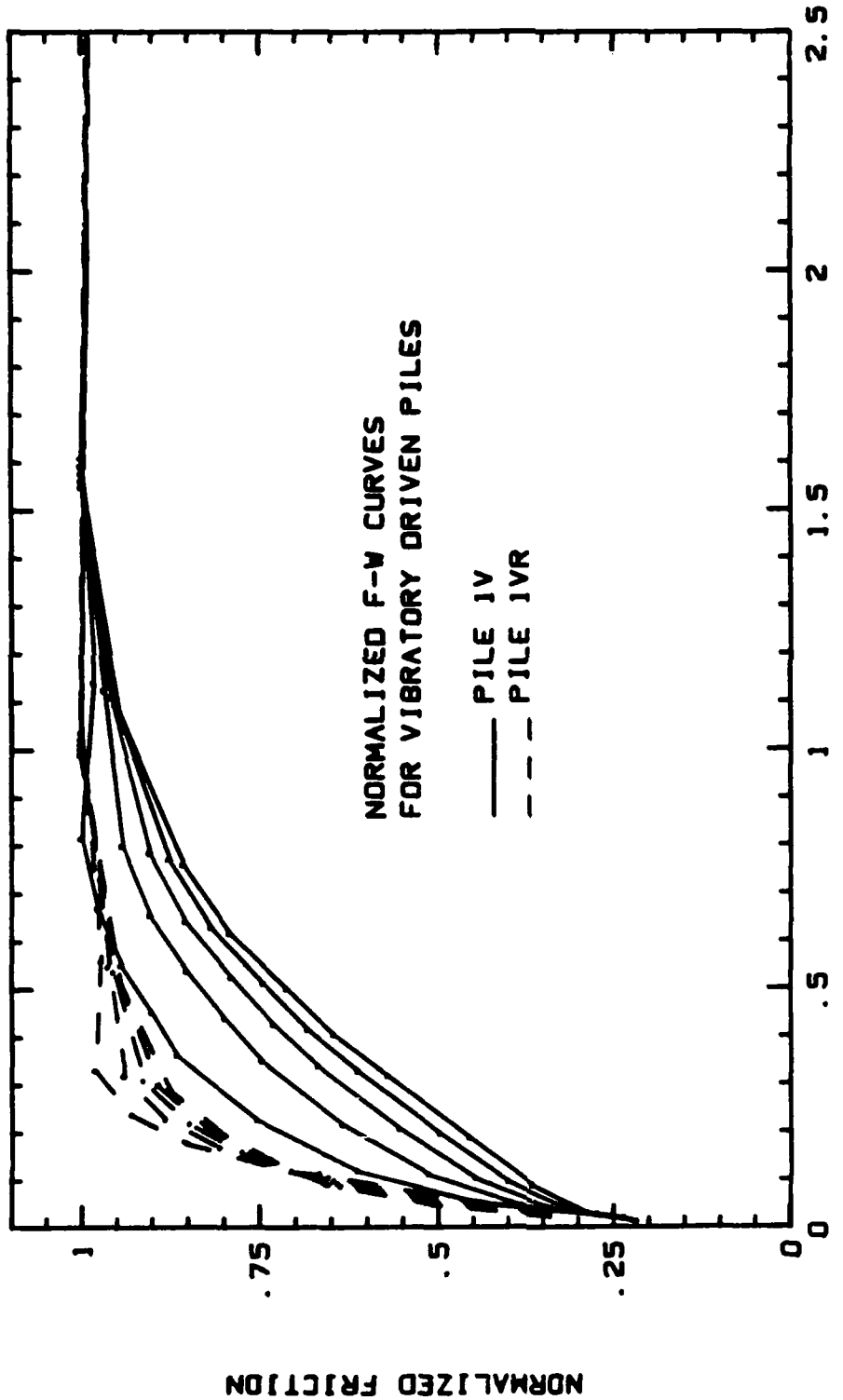

Figure 48. Normalized Friction Transfer Curves for Vibratory Driven Piles

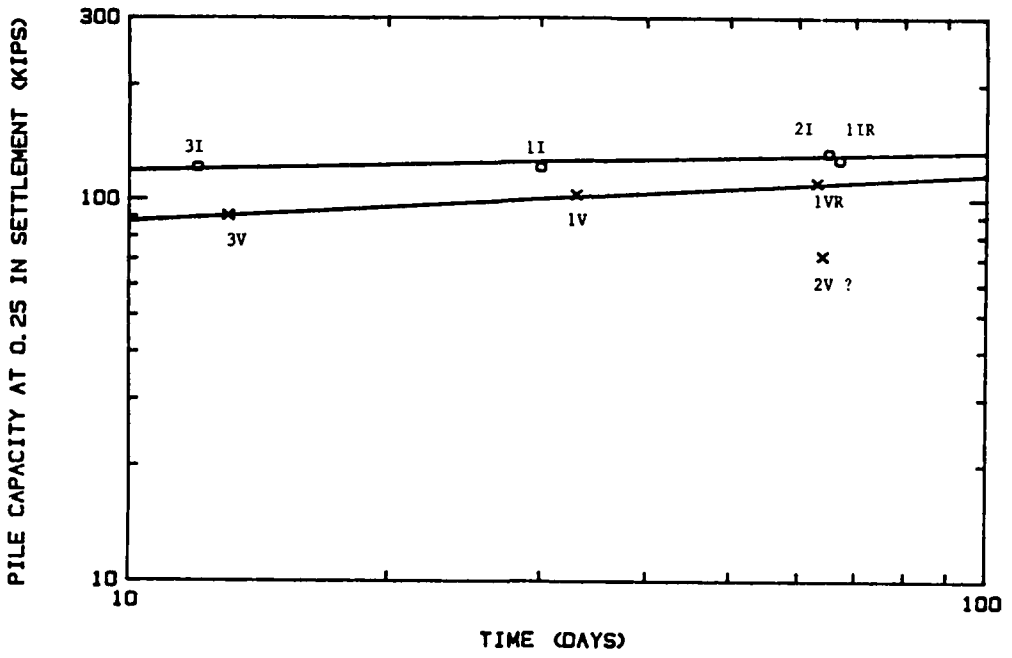

Figure 49. Pile Capacity at 0.25 in Settlement Versus Time

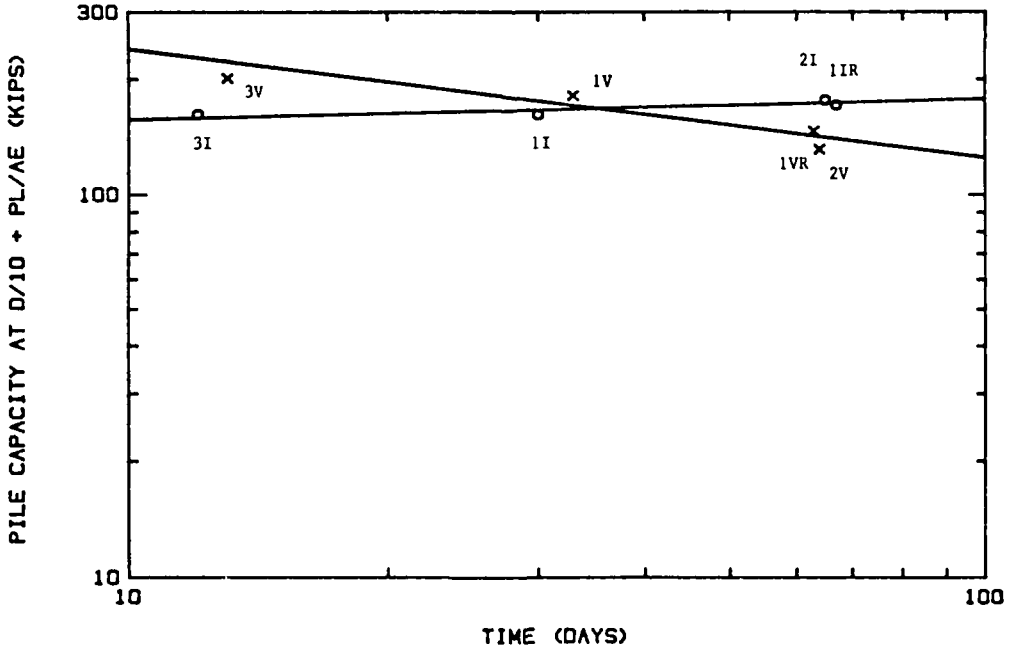

Figure 50. Pile Ultimate Capacity Versus Time

Dam 26 had an average of 7.5% passing the #200 sieve while the sand at Hunter's Point had 0% passing the #200 sieve.

In the case of Hunter's Point several factors influence the change of capacity, one of which is the effect of time. The others include the influence of soil heterogeneity and the influence of the first load test on the second load test. In order to isolate the effect of time one solution would be to use integrity testing to obtain the variation of stiffness versus time. Another solution would be to use a series of load tests more closely spaced in time performed on the same pile over a longer period of time (eg. 1 day, 4 days, 15 days, 40 days, 100 days).

CONCLUSIONS AND RECOMMENDATIONS

The main conclusions to be drawn from this study are the following:

- Vibratory driving of piles leads to approximately the same maximum load at large displacements, but to a larger settlement at working loads.
- The load distribution is influenced greatly by the driving process. For the piles in this study, impact driving led to a point resistance which was 51% of the total load at maximum loading compared to 13% for vibratory driving.
- The load transfer curves are also affected by the driving process. Vibratory driving led to load transfer curves which required much larger movements to reach maximum loading. This accounts for the first conclusion above regarding larger settlements at working loads being observed for vibratory driven piles.
- The effects of vibratory driving listed above are lessened upon reloading of the pile. Upon reloading, a vibratory driven pile carries a larger percentage of the load in point resistance (29%) and the load transfer curves take on the same shape as the impact driven piles.
- The data show that for impact driven piles there is a trend towards a slight increase in capacity versus time. For vibratory driven piles however, the data does not show any clear trend.

The following recommendations are made based on the results of this study:

- A series of load tests should be performed in a natural sand deposit to verify the results found in this study. The test program should include longer piles (at least 50 ft long) to determine if the same behavior occurs.
- An attempt should be made to load test piles which have been installed with a vibratory hammer and then tapped with an impact hammer. This procedure may yield the speed of installation of the vibratory hammer with the stiffer initial response of the impact driven piles.
- In order to isolate the effect of time on the variation of the pile stiffness response integrity testing could be used. This would have the advantage of being performed on the same pile, and the loads are small enough not to change the soil structure around the pile.
- In order to isolate the effect of time on the variation of the pile capacity a series of load tests more closely spaced in time performed on the same pile over a longer period of time. For example, a series of tests could be performed at 1 day, 4 days, 15 days, 40 days and 100 days after driving. This would have the advantage of being performed on the same pile and would include enough load tests to be able to assess the effect of one load test on subsequent load tests.

REFERENCES

Holloway, D.M., "Dynamic Monitoring Program Results, FHWA Vibratory Hammer-Pile Testing, Hunters Point, California," Report to Geo/Resource Consultants, 1987.

Hunter, A.H., Davisson, M.T., "Measurements of Pile Load Transfer," Performance of Deep Foundations, ASTM STP 444, American Society for Testing and Materials, 1969, pp. 106-117.

Ng, E.S., Briaud, J.-L., Tucker, L.M., "Pile Foundations: The Behavior of Piles in Cohesionless Soils," FHWA Report FHWA-RD-88-080, 1988.

Ng, E.S., Briaud, J.-L., Tucker, L.M., "Field Study of Pile Group Action in Sand," FHWA Report FHWA-RD-88-081, 1988.

Rausche, F., Goble, G.G., Likins, G.E., "Dynamic Determination of Pile Capacity," Journal of Geotechnical Engineering, ASCE, Vol. 111, No. 3, March 1985.